MONSOON AND THE GENERAL CIRCULATION OF THE TROPICS IN JUNE-AUGUST

by

Zen-Kay Jao

B.S., Taiwan Provincial Cheng-Kung University (1965)

SUBMITTED IN PARTIAL FULFILLMENT OF THE REQUIREMENTS FOR THE DEGREE OF MASTER OF SCIENCE

at the

MASSACHUSETTS INSTITUTE OF TECHNOLOGY

December 23, 1970 (i.e. Feb. 1971)

Signature of Author _____
Department of Meteorology, Dec. 1970

Certified by _____
Thesis Supervisor

Accepted by _____
Chairman, Department Committee on Graduate Studies

MONSOON AND THE GENERAL CIRCULATION OF THE TROPICS IN JUNE-AUGUST

by

Zen-Kay Jao

Submitted to the Department of Meteorology on December 23, 1970
in partial fulfillment of the requirements for the degree
of Master of Science

ABSTRACT

The latent heat release associated with the large precipitation in the monsoon region produces the highest mean temperature at a given pressure level in the tropics and also preduces a large vertical motion in this region. One Walker cell is found in the Indian monsoon region with the center of the cell close to 80E. It is also suggested that the two wave pattern in the extratropical region in June-August is generated by the dynamical deflection of the zonal current passing over mountains.

Comparsion of the continuity equation and the first law of thermodynamics which are used to evaluate the mean vertical motion indicated that the second one is not a good method. The adiabatic method, neglecting the diabatic heating rate in the first law of thermodynamics, can't be used to evaluate the mean vertical motion in the tropics. All the large scale vertical motion used in this study is derived from the continuity equation. The horizontal transport of Ω-angular momentum is assumed to be zero across any latitude circle but is one or two orders of magnitude larger than the relative angular momentum transport in any limited regions in the tropics. The largest southward transport of Ω-angular momentum is found in the Indian monsoon region. The vertical transport of angular momentum across a given pressure level is mainly due to the Ω-angular momentum transport. The largest vertical transport of angular momentum in the tropical region in June-August is located in the monsoon region.

The mean kinetic energy of the whole column of atmosphere in the monsoon region is about 4×10^8 ergs cm^{-2} which is four times larger than other regions at the same latitude in the tropical region. The large mean kinetic energy in the monsoon region is primarily maintained by the horizontal pressure gradient force against the large mean kinetic energy dissipation. The mean kinetic dissipation in the monsoon region is about 900 ergs $cm^{-2} sec^{-1}$ which is larger than the mean kinetic energy dissipation for the whole tropical region, the latter value being about 340 ergs $cm^{-2} sec^{-1}$.

Thesis Supervisor: Reginald E. Newell

Title: Professor of Meteorology

TABLE OF CONTENTS

CHAPTER 1

INTRODUCTION

The word monsoon is derived from the Arabic word for 'season'; it was applied by seamen navigating over the Arabian sea and the Indian ocean to the annual seasonal alternation of winds. It is now generally applied to the predominant air currents with a marked seasonal shift which cause the large quasi-stationary deviations from the zonal mean average flow in the tropics. They are developed in the summer season of either hemisphere but the Asiatic monsoon is the best known of the monsoons. Extensive seasonal heavy rainfall is observed in India, Southeast Asia and adjoining seas over a large range of latitudes and longitudes.

The latent heat release associated with the large precipitation in this monsoon region produces the highest mean temperatures and the lowest mean geopotential heights at a given pressure level in the tropics. A strong easterly wind in the upper troposphere in summer is a special feature of the Asiatic and Australian monsoons and is not found over the Atlantic or the Pacific monsoon regions. The longitudinal asymmetry of the monsoon has a significant influence on the general circulation of the atmosphere in the tropics.

The purpose of the present study is to examine the influence of the Asiatic monsoon on the general circulation, therefore the study here is restricted to June-August in the tropics. The data sources are given in Chapter 2. In Chapter 3 an intense Walker circulation is found in the Indian monsoon region with the center of the cell close to 80E. The strength of this Walker circulation is about the same as the Hadley cell circulation for the same width along a given latitude and longitude respectively. It is also suggested that the two wave pattern in the extratropical region in June-August is generated by the dynamical deflection of the zonal current passing over mountains which produces a large southward motion in the monsoon region. The dynamical deflection in June-August may be intensified by the superposition of the geostrophic wind produced by the land and sea distribution. In Chapter 4 the methods used to calculate the large scale vertical motion are discussed. Kyle (1970) has found there is a large vertical motion over the monsoon region with the use of the continuity equation to calculate $\overline{\omega}$ in the tropical region. A comparision of the continuity equation and the first law of thermodynamics which were used to evaluate $\overline{\omega}$ indicates that the second one is not a good method. The longitudinal variation of the angular momentum transport is presented in Chapter 5. In the horizontal transport, the Ω-angular momentum

transport is assumed to be zero across any latitude circle but it is one or two orders of magnitude larger than the relative angular momentum transport in any limited region in the tropics. The largest southward transport of Ω -angular momentum is found in the Indian monsoon region. The vertical transport of angular momentum is mainly due to the Ω -angular momentum transport. Finally in Chapter 6 the relative importance of each term in the mean kinetic energy budget is presented. The mean kinetic energy in the monsoon region is about four times larger than in other regions at the same latitude in the tropics. The mean kinetic energy dissipation in the monsoon region is about 900 ergs/cm^{2}sec which is larger than the mean kinetic dissipation for the whole tropical region, the latter value being about 340 erg/cm^{2}sec. The large mean kinetic energy in the monsoon region is primarily maintained by the horizontal pressure force against the large mean kinetic energy frictional dissipation.

Most of these studies except Chapter 6 have examined the long term mean (July 1957 to December 1964) and each separate year from 1960 to 1963. There is some year to year change but this variation is much smaller than the seasonal change. No significant year to year changes have been found; therefore all the studies for separate years are not discussed here.

CHAPTER 2

DATA

Most data used in this study were collected by R. E. Newell, J. W. Kidson and J. M. Wallace. A detailed explaination of the data and its sources can be found in chapter 2 of Newell et al (1970). More than three hundred radiosonde and radar wind stations within the overall period July 1957 to December 1964 covered an area from 45N to 45S. Mean zonal wind $\overline{u}$, mean meridional wind $\overline{v}$, mean temperature $\overline{T}$, mean geopotential $\overline{Z}$, the covariances $\overline{u'v'}$, the standard deviation $\sqrt{\overline{u'^2}}$ and $\sqrt{\overline{v'^2}}$ as well as others but not used here were computed for four three-month seasons: December-February, March-May, June-August and September-November. Most of the tropical data within the troposphere were processed by J. W. Kidson and R. S. Crosby. Many stations did not report regularly throughout the entire period so that the quantity and quality of the data varied considerably between stations. The principle reporting time was 0000 GMT but where necessary data at 0600 and 1200 GMT were included to improve the coverage. Nine standard levels 1000 850, 700, 500, 400, 300, 200, 150 and 100 mb are used. At each level maps are drawn and hand analyzed and grid points are read at 10 degree intervals in latitude, and 20 degree intervals in longitude from 40N to 30S and from 180W to 160E.

CHAPTER 3

ZONAL AND MERIDIONAL WIND FIELD

3.1 Zonal Wind

The main feature of the $[\bar{u}]$ cross section (Newell et al 1970) in June-August is the easterly wind between 25N and 15N separating two familiar westerly regions, the axis of the westerly jet in the Northern Hemisphere is further north than 40N and the westerly jet in the Southern Hemisphere is located at 30S-35S with the maximum velocity about 30 m/sec. But $[\bar{u}]$ can't tell us the real story because of the presence of longitudinal asymmetries in the $\bar{u}$ fields as shown in longitudinal cross sections. Figures (3.1) to (3.7) present the longitudinal profile of $\bar{u}$ along 40N, 20N, 10N, 00N, 10S, 20S and 30S taken from Newell et al (1970).

There are westerlies at all levels on middle latitudes with a maximum reaching 45 m/sec at 30S, 130E. In the equatorial zone the Western Hemisphere is also characterized by upper level westerlies with easterlies below. In the Eastern Hemisphere the predominant feature is strong easterlies in the upper troposphere accompanying the Indian monsoon. Newell et al(1970) pointed out the increase of easterly wind with height in the monsoon region; according to the thermal wind relationship, this implies that the

temperature increases away from the equator and that the middle levels have a stronger temperature gradient from higher latitudes toward the equator.

The maximum easterly velocity in the monsoon region is about 30 m/sec at 15N, 70E and the region of easterlies extends from 25N to 15S over the Eastern Hemisphere. This monsoon circulation is one of the most important stationary disturbances in the tropics. The summer monsoon not only generates a strong Hadley circulation but also generates a strong Walker circulation in the tropics. Walker and Bliss (1932) have described a pressure anomaly pattern in both the Eastern and Western Hemispheres; their statistical expression reflects a certain larger scale exchange of air between the Eastern and Western Hemispheres. This is known as the Walker circulation or southern oscillation. The streamlines along 25N and 15N are given in Figures (3.8) and (3.9). The vertical velocity is calculated from the continuity equation, a discussion is given in Chapter 4. The direction of streamline is determined from $\theta = \tan^{-1} \frac{M\bar{W}}{\bar{u}}$ where $\bar{W}$ is the mean vertical velocity, $\bar{u}$ is the zonal mean velocity, M is a constant determined by the ratio of horizontal scale and vertical scale in Figure (3.8). From these streamlines pattern, one intense Walker circulation is found in the warm Indian monsoon region. The latent heat released in the monsoon region generally

contributes to the rising motion from the Eastern Pacific to 80E with the maximum upward motion at 100E where the largest amount of rainfall occurs. The center of the Walker cell is close to 80E in the monsoon region. Downward motion occurs over the North Atlantic ocean and North Africa. The mass flux along 15N for 10 degree latitude belt in June-August is presented in Figure (3. 10), the strength is about 30×10^{12} gm/sec which is about the same as the strength of the Hadley cell in a separate meridional cross section of the same width.

3.2 Meridional Wind

The mean meridional wind component is very difficult to obtain from direct measurements. The mean meridional wind is small and is often exceeded by the daily variations. There are several methods of obtaining the mean meridional wind. In general they can be divided into: (a) indirect methods wherein the mean meridional wind is computed from the momentum, continuity and the thermodynamic equations; (b) direct methods wherein the mean meridional wind is obtained as a statistical average over a long period of daily observations. Only the zonal mean meridional wind can be obtained from the indirect method but in this study the main purpose is to examine the longitudinal asymmetry of the general circulation. Therefore the mean meridional winds in this study are

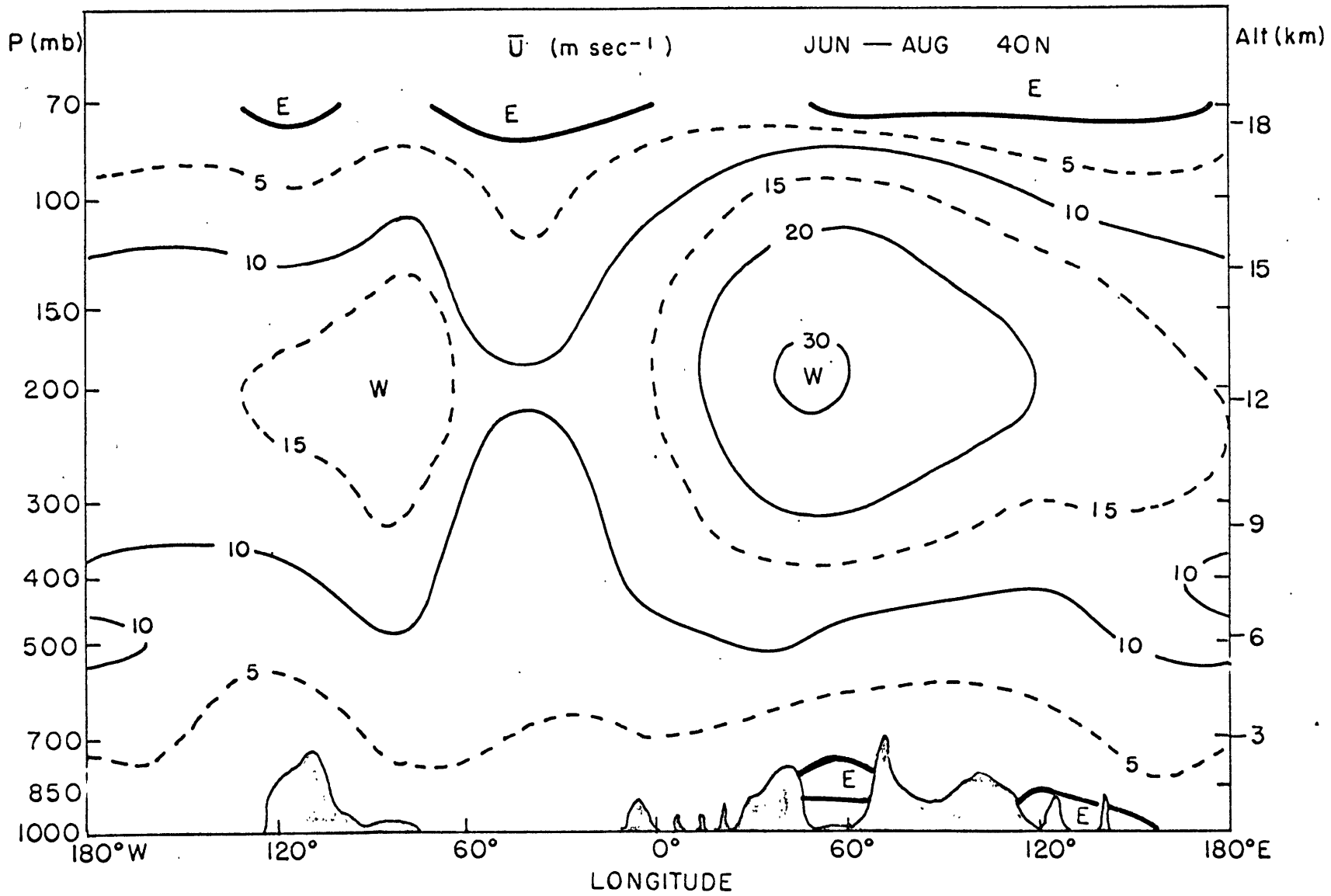

Figure 3.1 Mean zonal wind along 40N in June-August

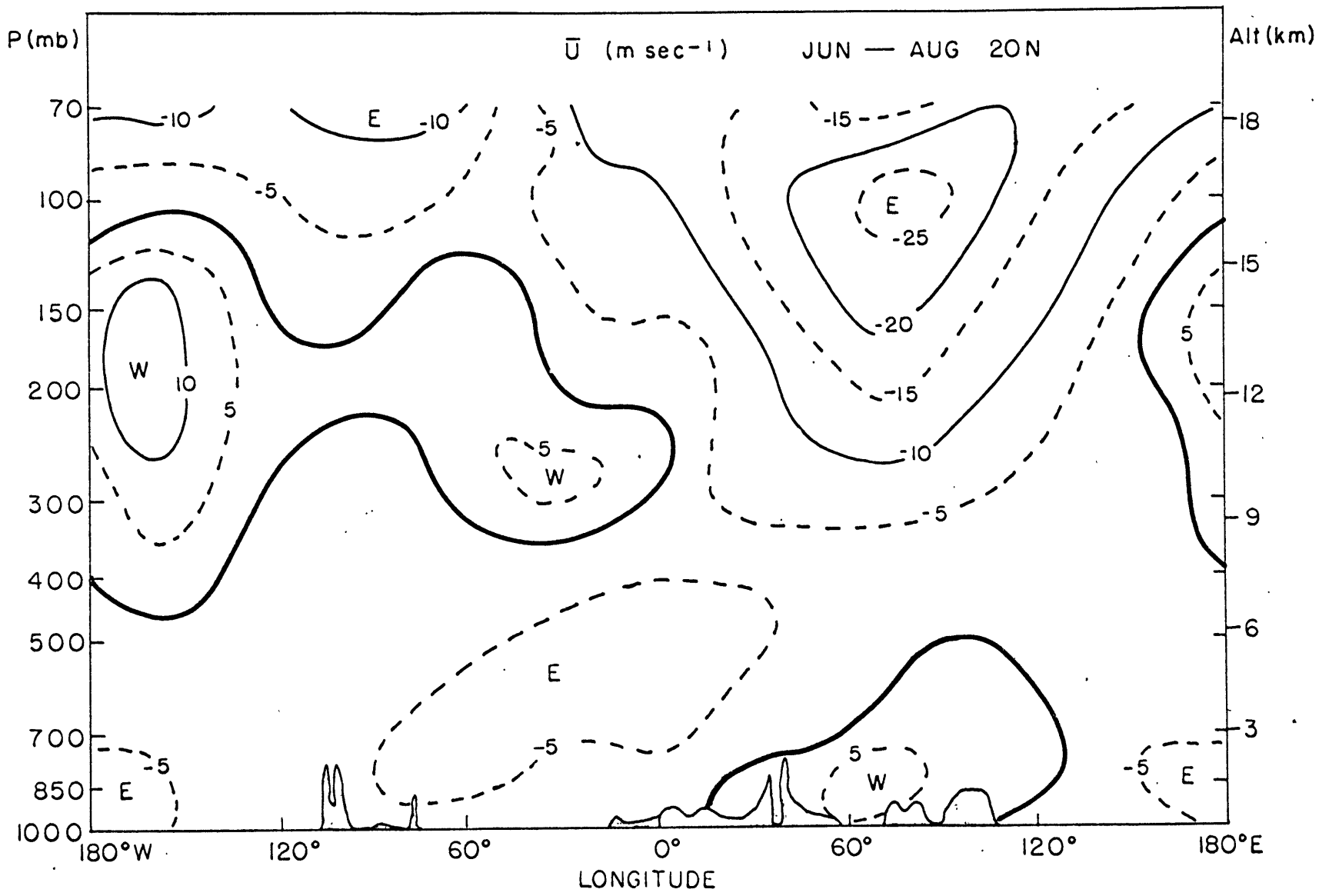

Figure 3.2 Mean zonal wind along 20N in June-August

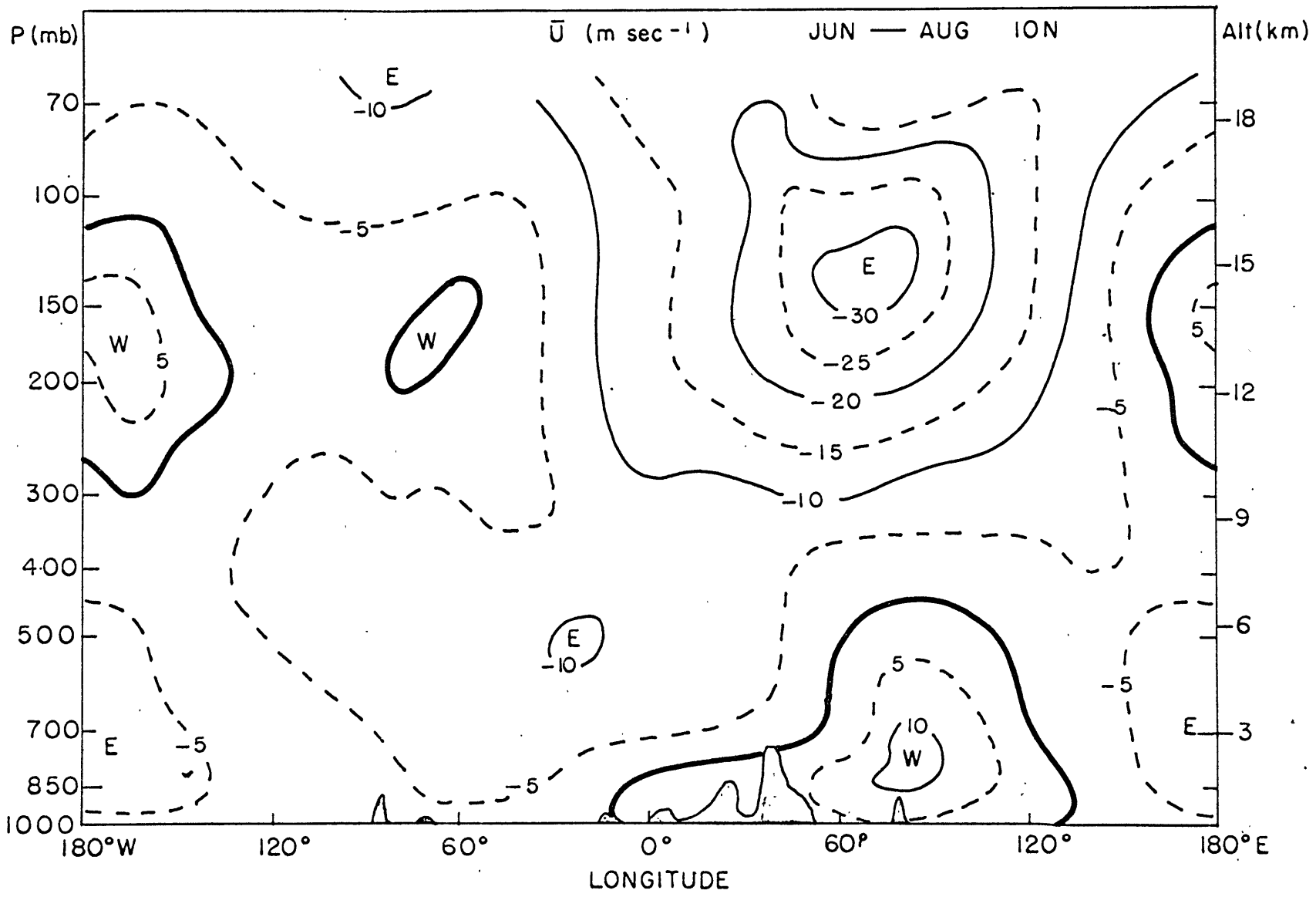

Figure 3.3 Mean zonal wind along 10N in June-August

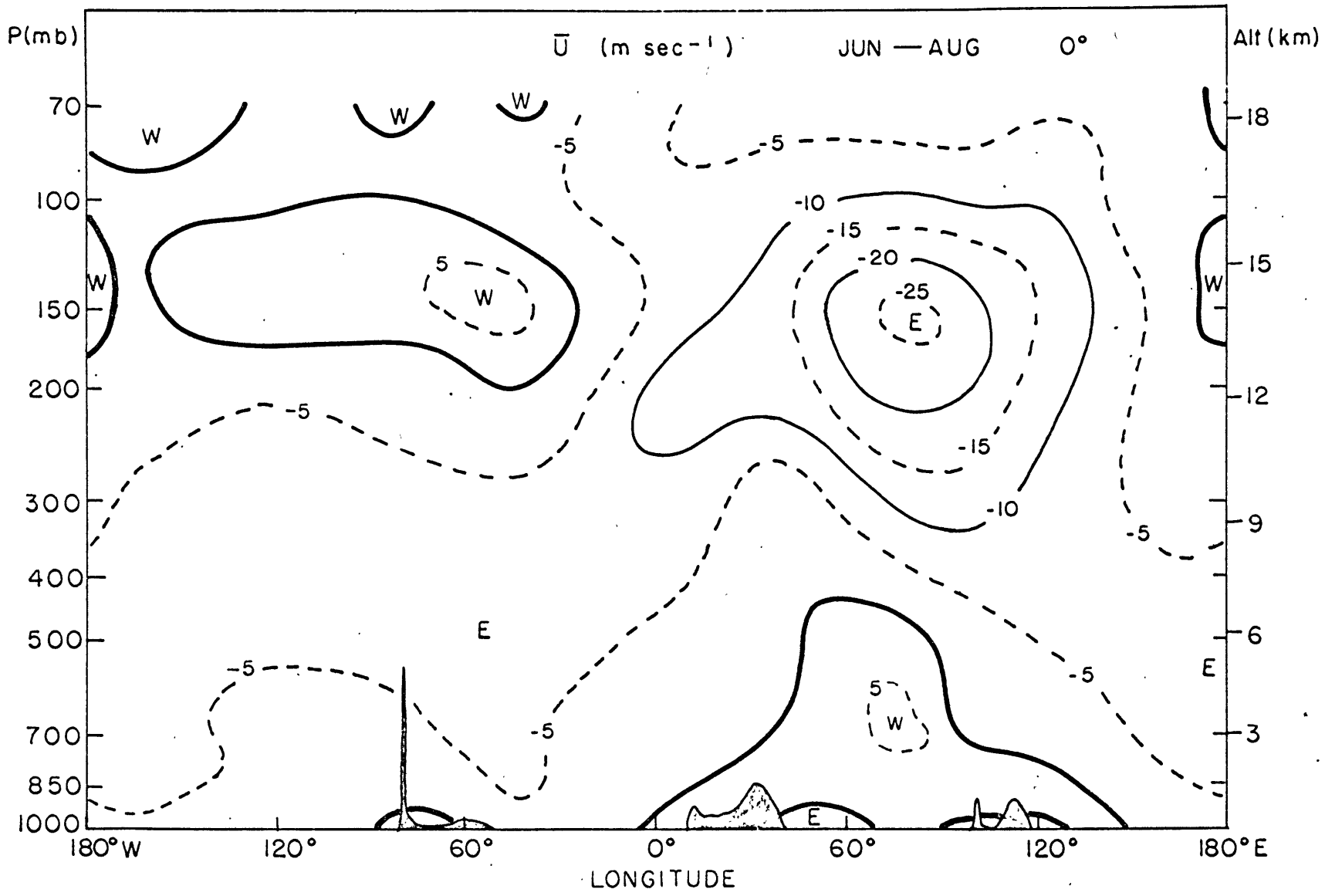

Figure 3.4 Mean zonal wind along equator in June-August

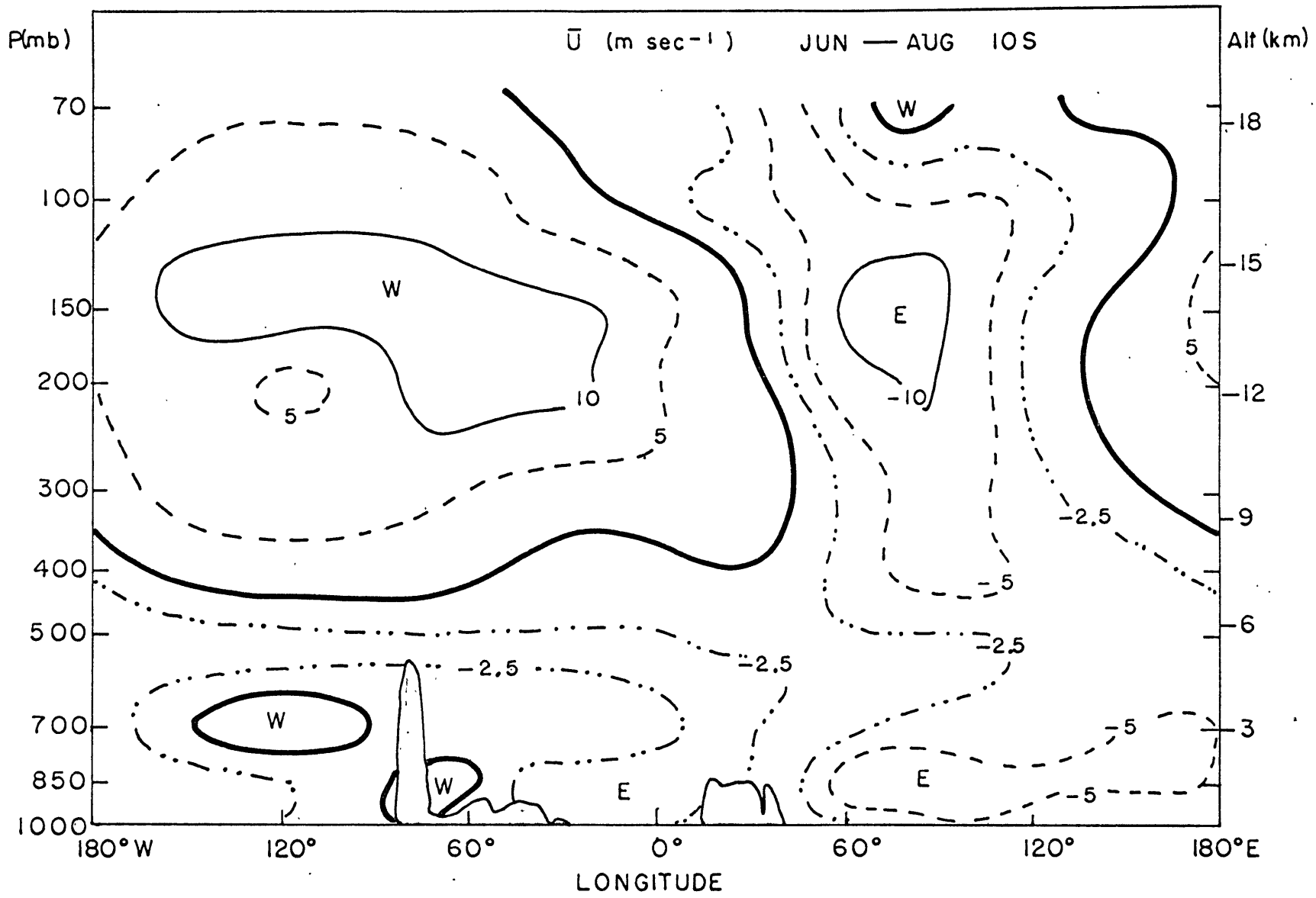

Figure 3.5 Mean zonal wind along 10S in June-August

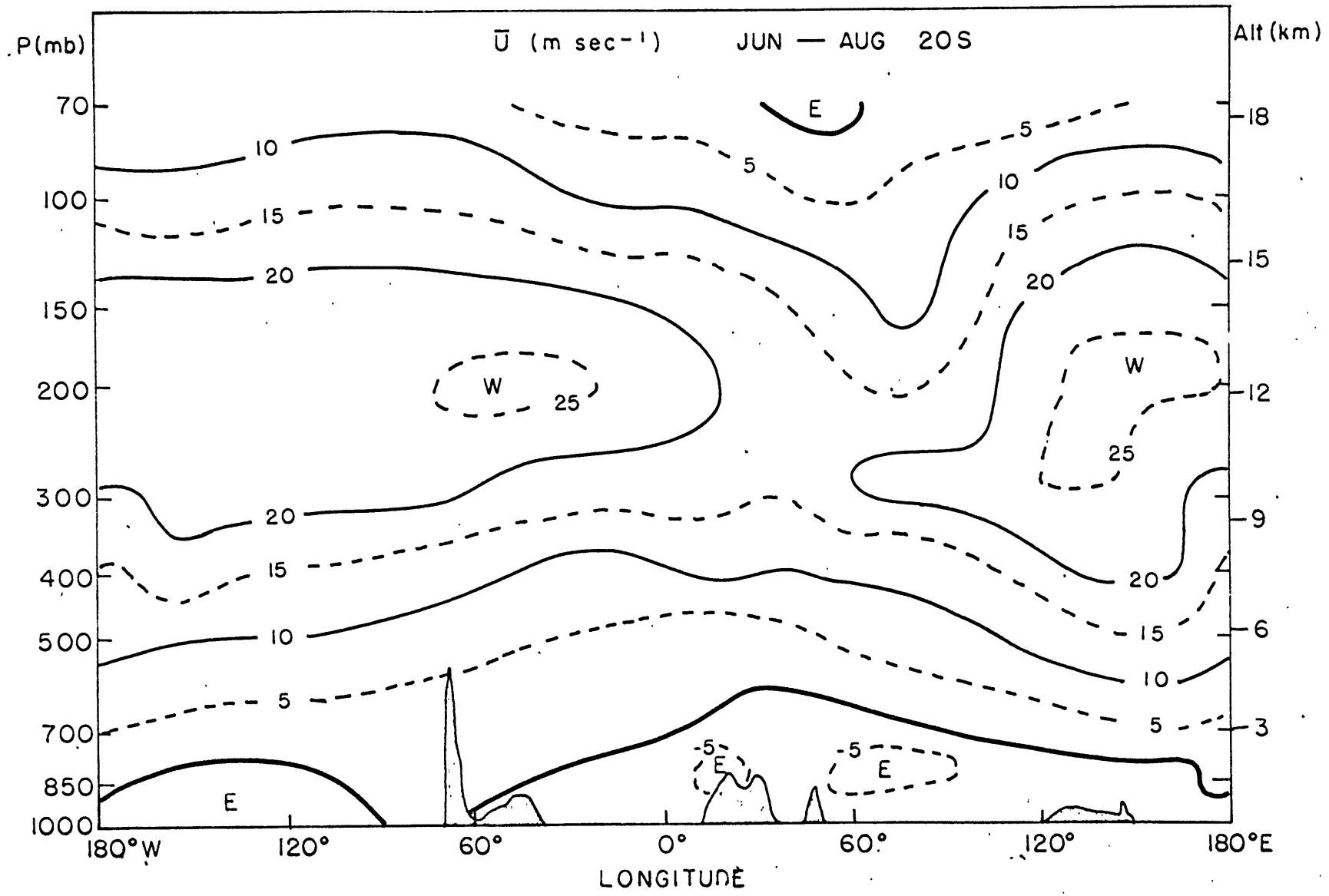

Figure 3.6 Mean zonal wind along 20S in June-August

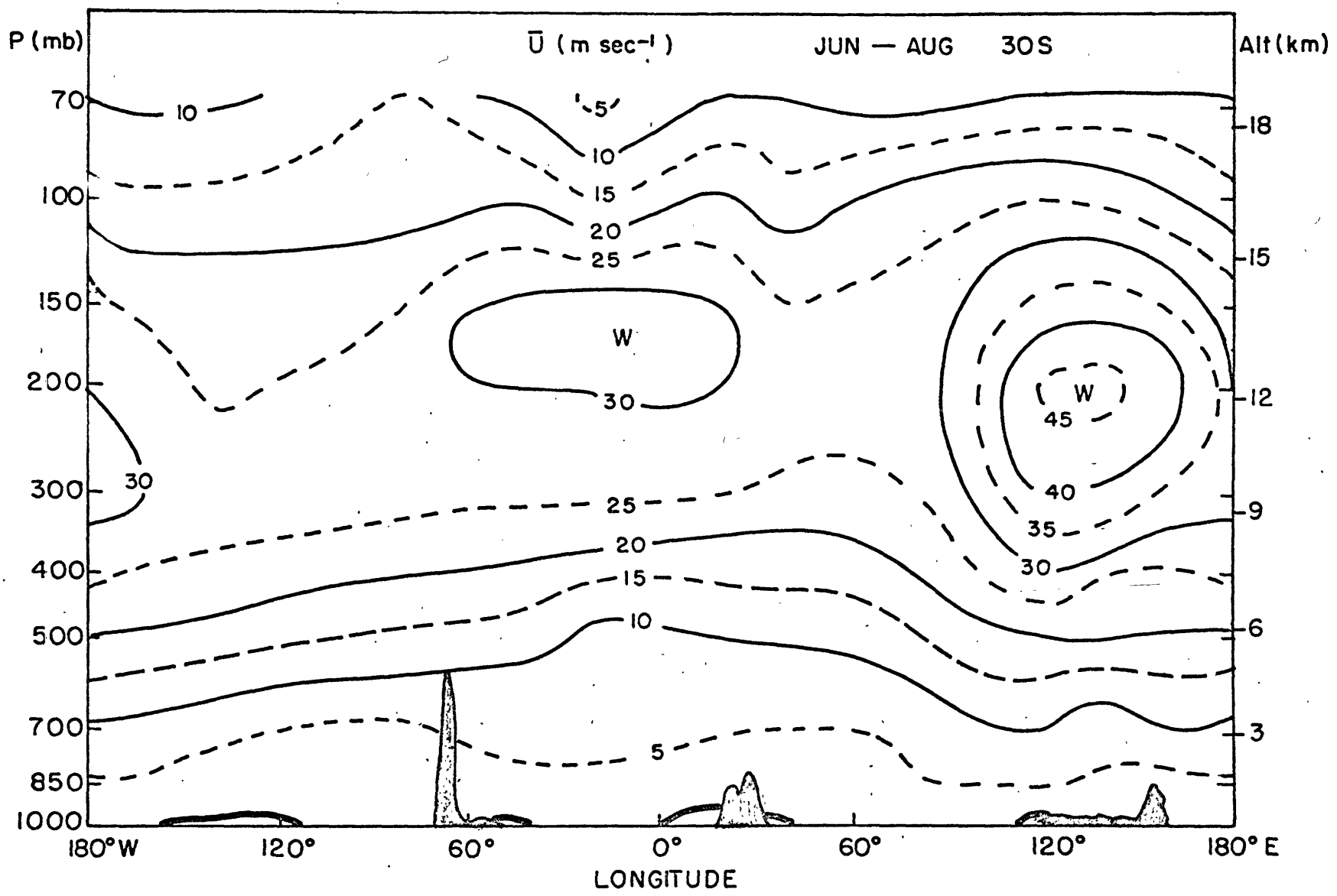

Figure 3.7 Mean zonal wind along 30S for June-August

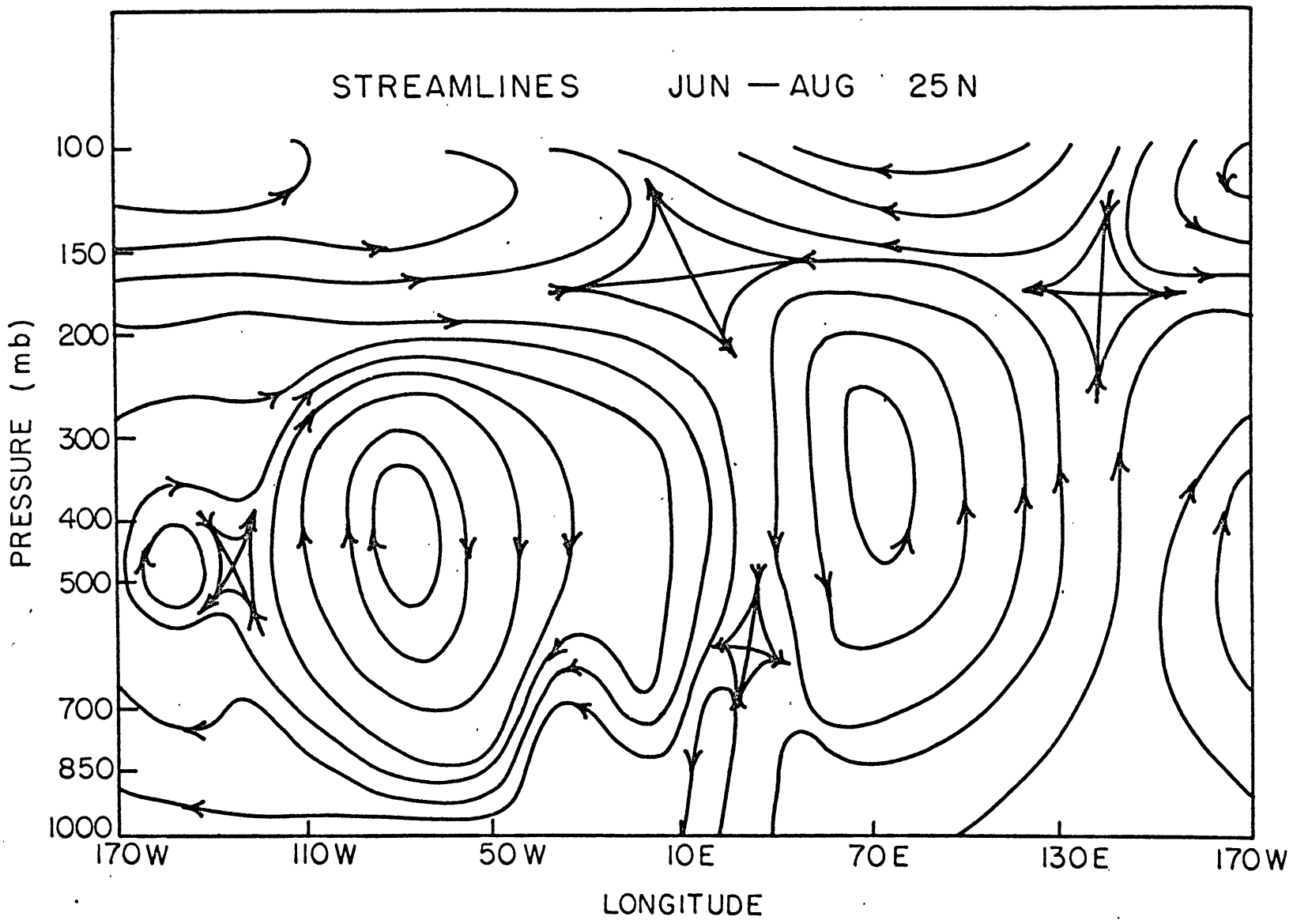

Figure 3.8 Streamlines along 25N in June-August

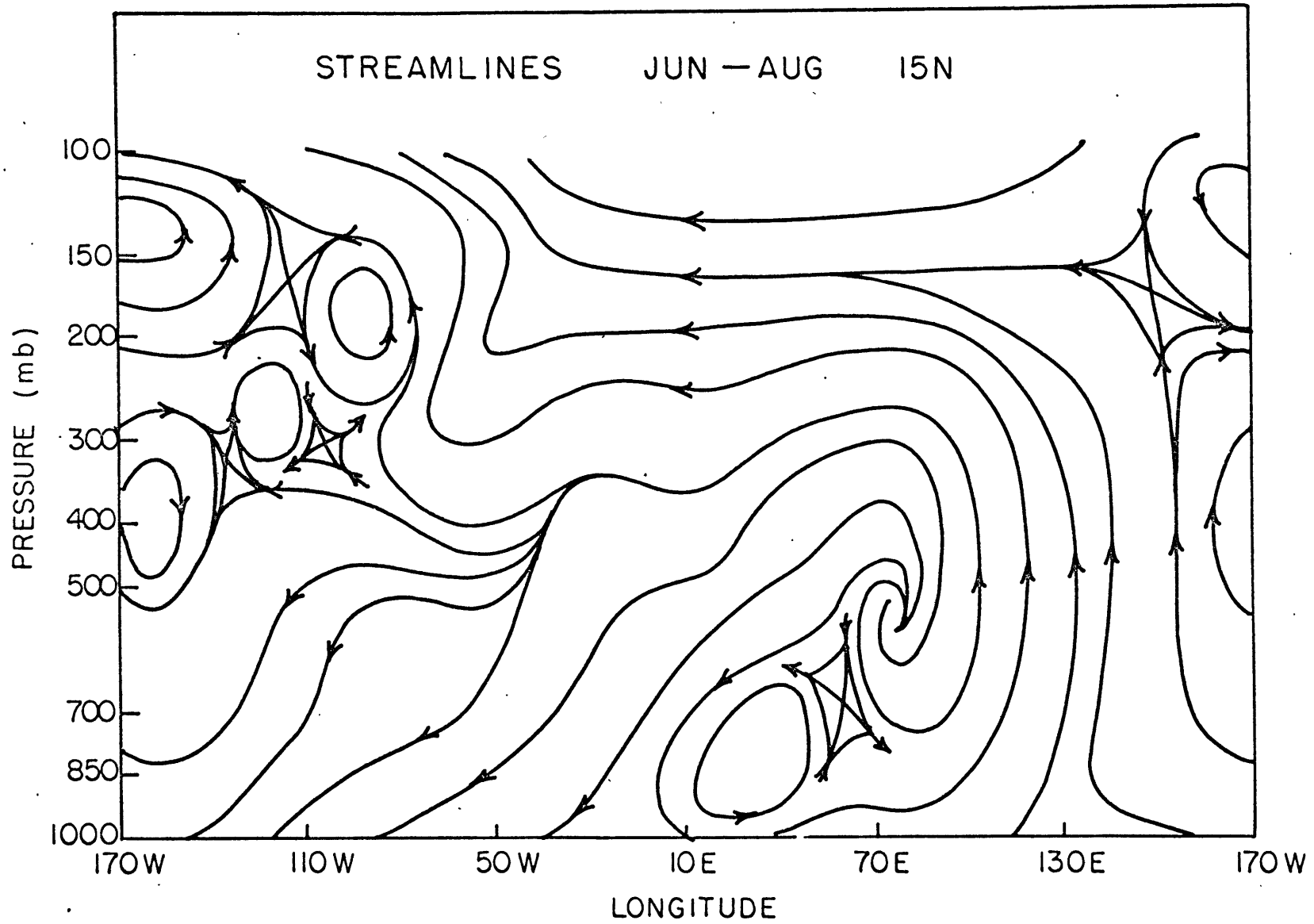

Figure 3.9 Streamlines along 15N in June-August

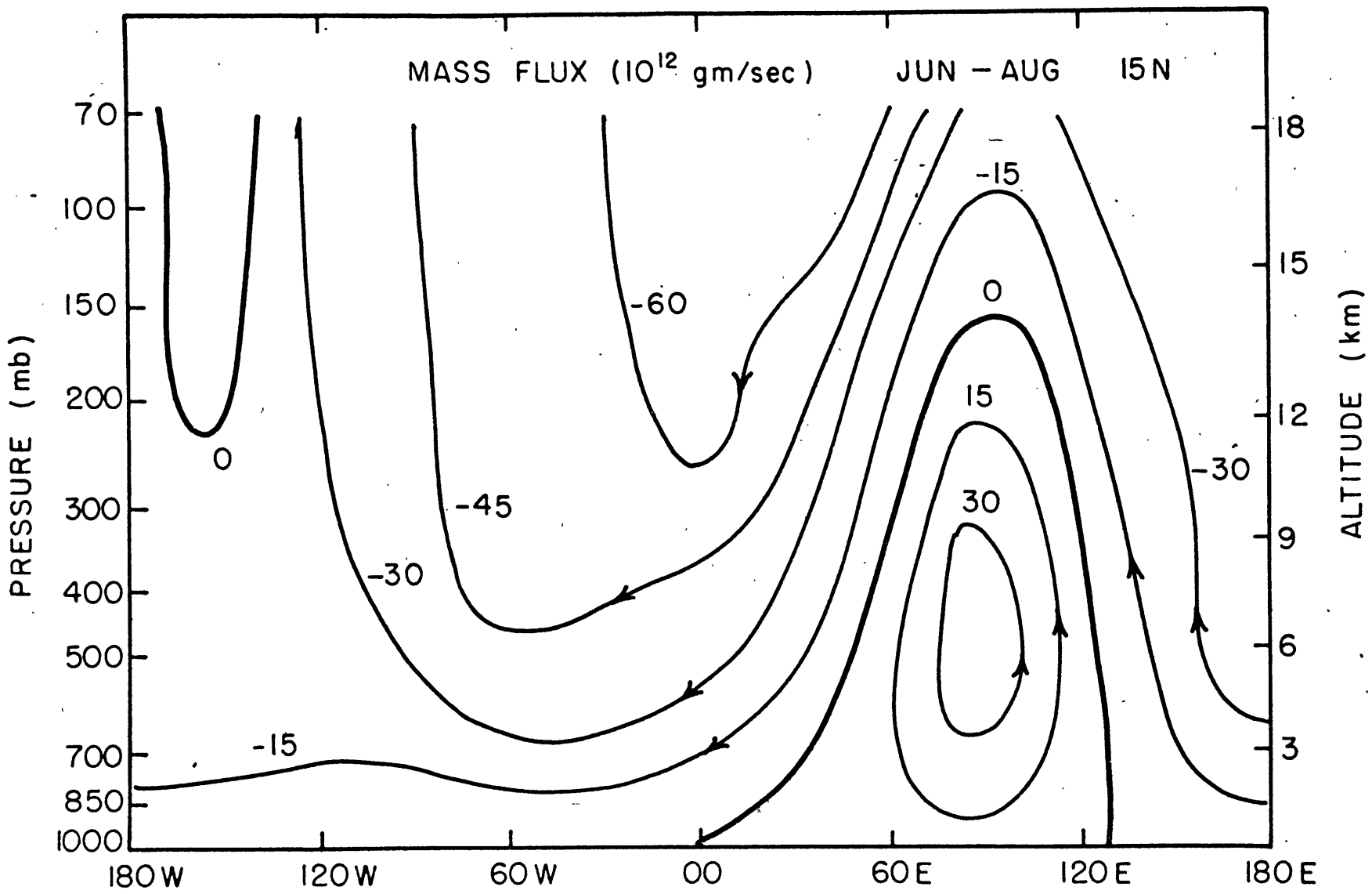

Figure 3.10 Mass flux along 15N for 10 degree latitude belt in June-August

obtained from observations rather than from indirect computations. The main feature of the $[\overline{v}]$ cross section is the Hadley cell circulation with southward flow in the upper troposphere and northward flow in the lower troposphere. The observed mean meridional velocity from 40N to 00N along each 10 degree latitude circle is presented from Figures (3.11) to (3.15) again taken from Newell et al (1970). The mean meridional velocity in the Northern Hemisphere in June-August shows two-wave pattern. These waves appear in the westerly flow at middle latitude and remain stationary or show only a slow motion. Burger (1959) in his famous paper on the scale analysis of planetary motion has pointed to the existence of these waves. Why are there two waves along a latitude circle in June-August ? In order to develop a complete theory, it is necessary to consider the thermal condition of the earth's atmosphere and the surface boundary condition which causes the deflection of large scale currents by mountain ranges.

In this chapter we wish to give a qualitive explanation of these quasi-stationary long waves in June-August. The thermal gradient in the summer hemisphere is not very large. It is suggested that the thermal influence in the Northern Hemisphere in June-August is of less importance than the dynamic effect of the mountains in causing these two-wave pattern in summer. When air currents ascend and descend large mountain barriers, they

must undergo lateral deflections of meandering. Bolin (1952) has considered this dynamic effect of the zonal current of a shallow inviscid homogenerous fluid of finite depth. Consider homogeneous barotropic inviscid horizontal flow in a rotating system on a β-plane in rectangular coordinate:

$$\frac{Du}{Dt} - fv = -g\frac{\partial h}{\partial x} \tag{3.2}$$

$$\frac{Dv}{Dt} + fu = -g\frac{\partial h}{\partial y} \tag{3.3}$$

and the incompressible continuity equation

$$\frac{\partial u}{\partial x} + \frac{\partial v}{\partial y} = \frac{-1}{H+h}\frac{D(H+h)}{Dt} \tag{3.4}$$

where h is the elevation of the free surface and H(x, y) is the depth of the atmosphere. Cross differentiation of equ. (3.2) and (3.3) then making the β-plane approximation gives:

$$\frac{D}{Dt}(\zeta+f) = -(\zeta+f)\left(\frac{\partial u}{\partial x} + \frac{\partial v}{\partial y}\right) + \left(\frac{\partial w}{\partial y}\frac{\partial u}{\partial z} - \frac{\partial w}{\partial x}\frac{\partial v}{\partial z}\right) \tag{3.5}$$

where $\zeta = \frac{\partial v}{\partial x} - \frac{\partial u}{\partial y}$, the vertical component of relative vorticity. It is then assumed that u and v are independent of z i. e. a barotropic atmosphere. By substitution of the incompressible

continuity equation (3.4) into (3.5) we get

$$\frac{D}{Dt}\left(\frac{\zeta+f}{H+h}\right) = 0 \qquad (3.6)$$

where h is usually negligible compared with H. This equation expresses the conservation of potential vorticity along a trajectory. Suppose there is uniform zonal flow over the mountain ridge independent of latitude with straight parallel where away from the mountains the fluid thickness is H_0, as shown in Figure (3.16). A quasi-stationary atmospheric long wave is nearly in a steady state, from equ. (3.6) is

$$\frac{\zeta+f}{H} = \frac{f_0}{H_0}$$

$$= \text{a constant along a streamline in steady flow} \qquad (3.7)$$

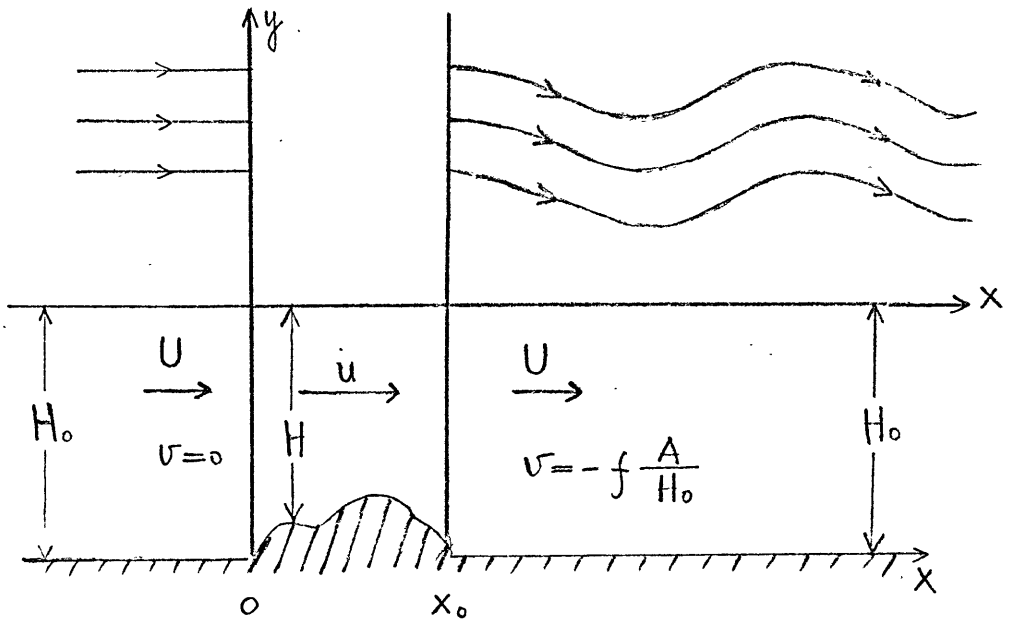

Fig. 3.16 The deflection effect of a mountain ridge on an incident uniform zonal flow

The x-component of the velocity is determined by the mass conservation equation

$$uH = UH_0 \tag{3.8}$$

and the y-component of the velocity is determined from equ. (3.7)

$$\zeta = \frac{dv(x)}{dx} = H\left(\frac{f_0}{H_0} - \frac{f}{H}\right) \tag{3.9}$$

where v is the perturbation velocity as the uniform zonal flow passes over the mountain. The velocity u is independent of y. If the zonal current deflection along each latitude if not too large we can assume $f \simeq f_0$. Integrating (3.9) gives:

$$v = f_0 \int_{-\infty}^{x_0} \frac{H - H_0}{H_0} dx \tag{3.10}$$

the whole cross section area of the mountain ridge is

$$A = \int_{-\infty}^{\infty} (H_0 - H)\, dx \tag{3.11}$$

substituting (3.11) into (3.10) gives

$$v(x_0) = -f_0 \frac{A}{H_0} \tag{3.12}$$

where $A > 0$, the effect of the mountain ridge is thus to deflect a westerly flow southward in the Northern hemisphere as the uniform zonal flow leaves the mountain ridge. On the downstream side the zonal current will return to its upstream value but the meridional velocity will change by an amount of $-\frac{f_c A}{H_0}$. Equ. (3.7) also shows

that the Rossby wave is generated as the flow leave the mountain. Assuming the atmospheric thickness is 10 km, the average height of the mountain ridge is 1 km and the width is 1000 km.

$$\frac{f_0 A}{H_0} \simeq \frac{10^{-5} \times 1000 \times 10^3 \times 10^3}{10 \times 10^3} \ m/sec$$

$$= 1 \ m/sec$$

This is in agreement with the fact that the observed mean meridional components are generally quite small and are of the same order of magnitude. From Figure (3.10) that mean meridional wind starts to deflect southward at 110W and 90E, just at the edge of the Rocky mountains and Himalaya mountains respectively. Maximum southward deflection of the meridional wind occurs at 110E with a magnitude of 6 m/sec in the extratropical region. This is due to the large mountains (the Himalayas and the Tibetian plateau) in this region. The average height of these mountains is about 5 km and the width is approximately 2000 km; from equ. (3.12), we get a maximum southward deflection of about 10 m/sec. From the above considerations the dynamic effect gives a satisfactory explanation of the planetary wave pattern in summer. South of the extratropical region, the strong monsoon easterlies destroys the two-wave pattern along each latitude circle. In winter, the temperature difference between the ocean and land is large. There always exists a low pressure

cyclonic center over the ocean and high pressure anticyclonic center over the continent in the low troposphere. The reverse is true in the upper troposphere. These cyclone and anticyclone structure superpose with the dynamic deflection of zonal flow passing over the mountains may cause the three-wave pattern in winter.

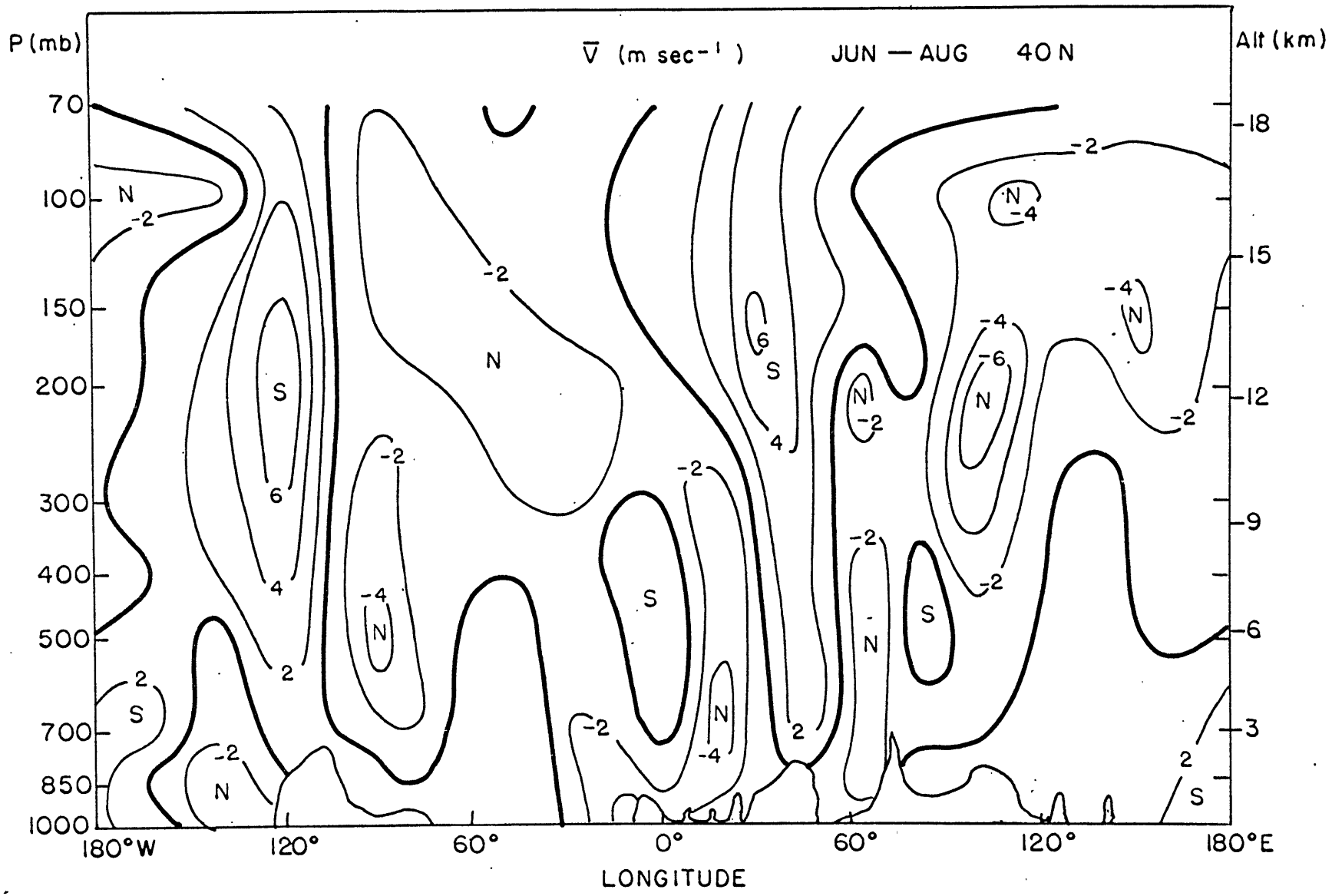

Figure 3.11 Mean meridional wind along 40N in June-August

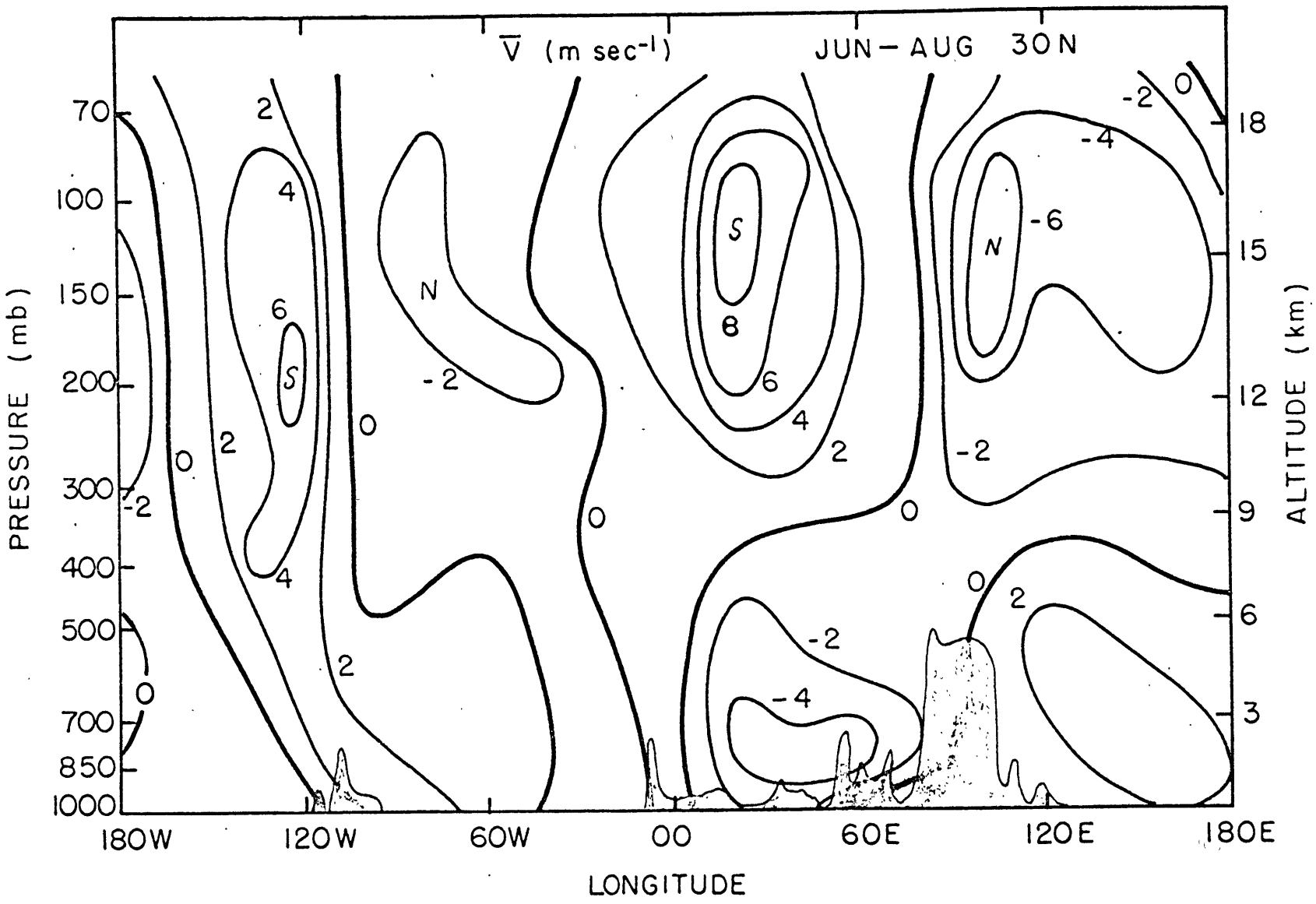

Figure 3.12 Mean meridional wind along 30N in June-August

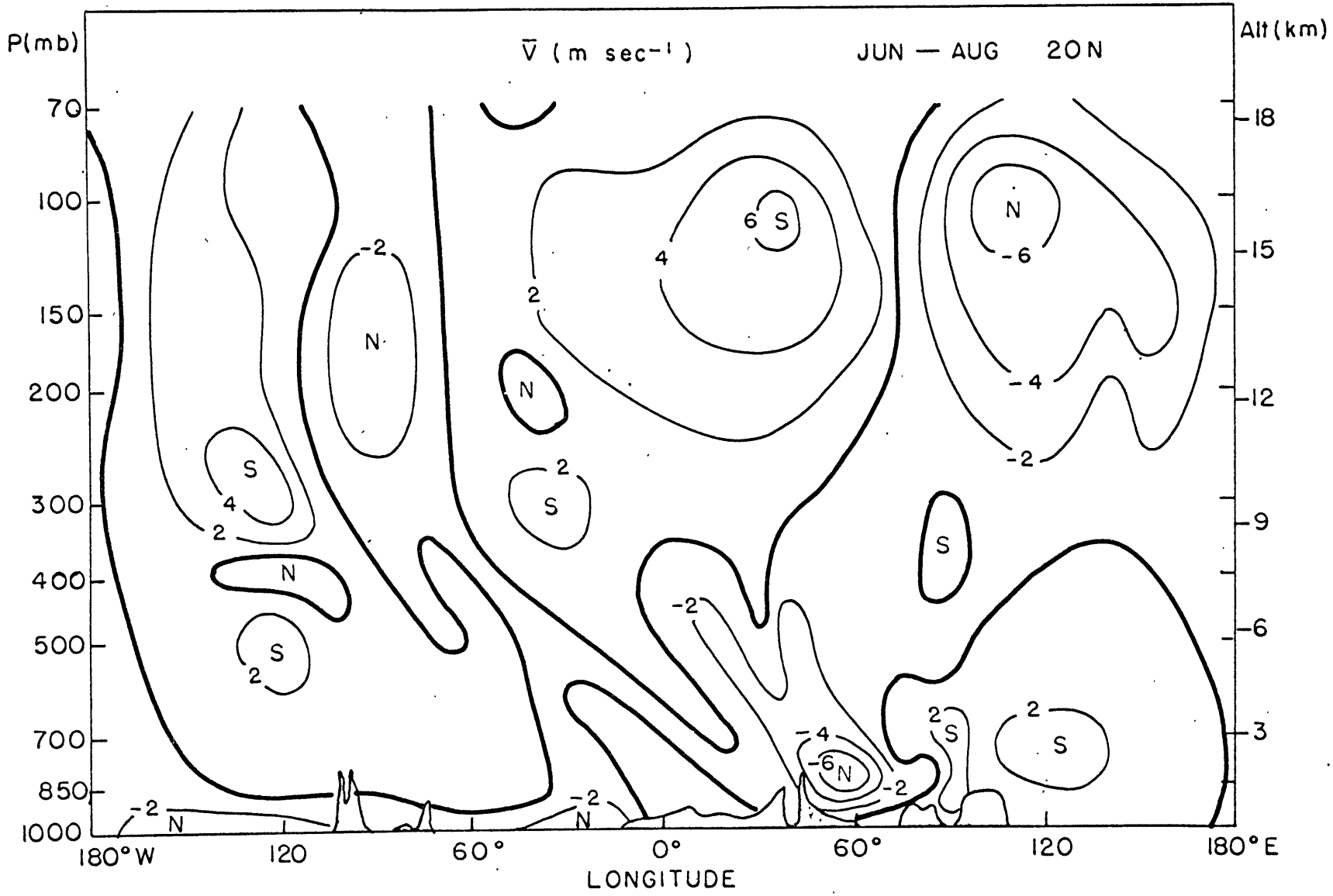

Figure 3.13 Mean meridional wind along 20N in June-August

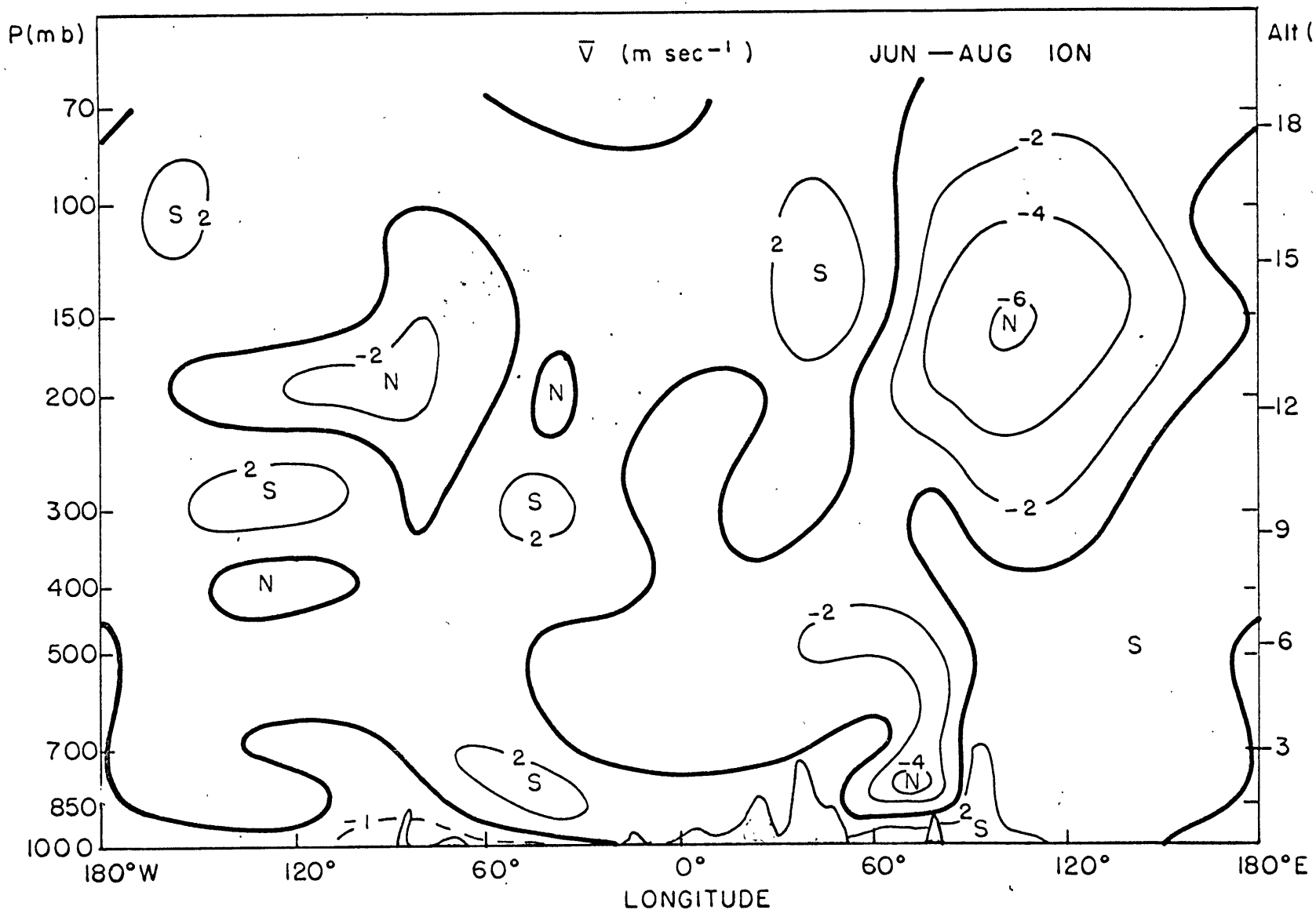

Figure 3.14 Mean meridional wind along 10N in June-August

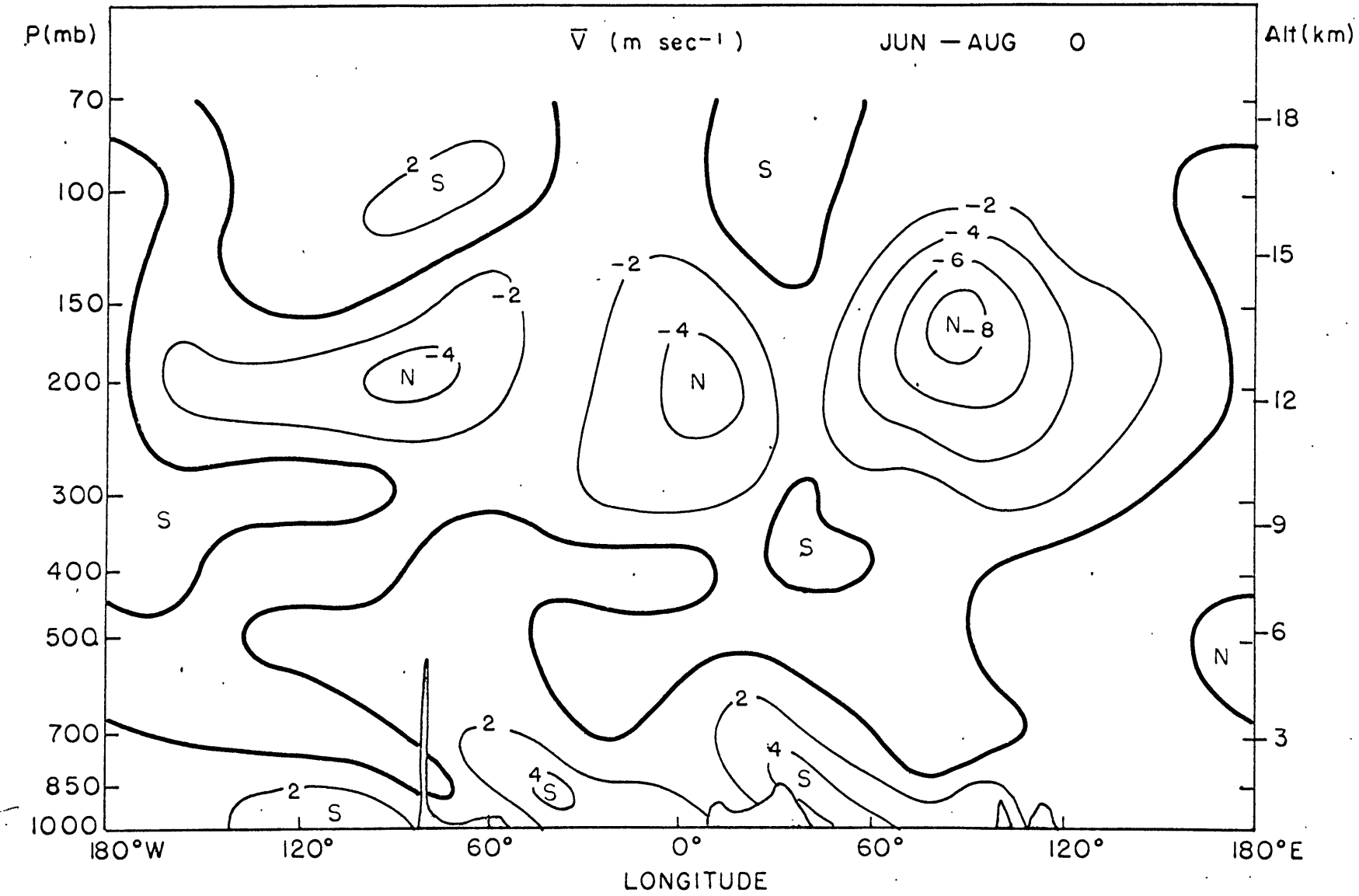

Figure 3.15 Mean meridional wind along equator in June-August

CHAPTER 4

METHODS OF COMPUTATION OF LARGE SCALE VERTICAL VELOCITY

The atmosphere large scale motion is nearly horizontal and the vertical velocity is too small to measure directly. But in many respects the vertical velocity is an important quantity, for it governs the rate of condensation and precipitation, which in turn has a large influence on the general circulation especially in the tropical region. Unfortunately vertical velocity can't be obtained from the routine daily observations and it can be obtained from indirect calculations.

There are several methods to calculate the vertical velocity: two exemples are the use of the continuity equation and the use of the first law of thermodynamics. Of course the accuracy of such computations for every method depends greatly upon the density of the aerological data and the quality of the observations. The main purpose of this chapter is to describe these methods with which the large scale vertical velocity can be computed. In these methods, $\overline{\omega}$ - the time averaged vertical velocity described in terms of pressure change, is calculated from $\overline{u}$, $\overline{v}$ and other observational quantities. The longitudinal asymmetry of these observational

data causes the asymmetry of $\overline{\omega}$.

4.1 $\overline{\omega}$ Calculated from the First Law of Thermodynamics

Changes in the atmosphere are governed by the laws of physics, which can be expressed in the form of certain differential equations, the relative importance of the differential terms involved in the process can be obtained from direct calculation. From the first law of thermodynamics

$$\frac{1}{c_p}\frac{dQ}{dt} = \frac{dT}{dt} - \frac{\alpha}{c_p}\frac{dp}{dt}$$

$$= \frac{\partial T}{\partial t} - V \cdot \nabla_p T + \omega\left(\frac{\partial T}{\partial p} - \frac{\alpha}{c_p}\right) \qquad (4.1)$$

where $\omega = \frac{dp}{dt}$ and $\frac{dQ}{dt}$ is the rate of net diabatic heating. The diabatic heating includes the infrared cooling, solar heating, latent heat release and turbulent transfer of sensible heat at the boundary layer.

There is net radiative cooling in most of the troposphere and latent heat release is the predominant heating source. If equation (4.1) is averaged over a certain time interval, the covariances of ω with other quantities are omitted and an uncentered finite difference method used, we obtain the finite difference equation of the first law of thermodynamics as:

$$\frac{\overline{T}^{n+1}_{ijk} - \overline{T}^{n}_{ijk}}{\Delta t} + \overline{u}^{n}_{i+\frac{1}{2},j+\frac{1}{2},k} \frac{\overline{T}^{n}_{i+1,j+\frac{1}{2},k} - \overline{T}^{n}_{i,j+\frac{1}{2},k}}{\Delta x}$$

$$+ \overline{v}^{n}_{i+\frac{1}{2},j+\frac{1}{2},k} \frac{\overline{T}^{n}_{i+\frac{1}{2},j+1,k} - \overline{T}^{n}_{i+\frac{1}{2},j,k}}{\Delta y}$$

$$+ \overline{\omega}_{i+\frac{1}{2},j+\frac{1}{2},k} \left(\frac{\overline{T}^{n}_{i+\frac{1}{2},j+\frac{1}{2},k+1} - \overline{T}_{i+\frac{1}{2},j+\frac{1}{2},k-1}}{2\Delta p} - \frac{\overline{\alpha}^{n}_{i+\frac{1}{2},j+\frac{1}{2},k}}{c_p} \right)$$

$$= P^{n}_{i+\frac{1}{2},j+\frac{1}{2},k} + R^{n}_{i+\frac{1}{2},j+\frac{1}{2},k} \qquad (4.2)$$

where P is the latent heat release and R is the net radiational cooling at given point in atmosphere. In order to compare $\overline{\omega}$ computed from equation (4.2) with the result from the continuity equation, only $\overline{\omega}$ at 500 mb is calculated. All data except the diabatic heating comes from the same source as mentioned in Chapter 2. The diabatic heating rate is the most difficult part to specify in using the thermodynamic equation. The precipitation indicates the latent heat release in the whole column of the atmosphere. The climatological data of precipitation in June-August are taken from World Weather Records (1966) and are shown in Figure (4.1). The vertical distribution of latent heat release is taken from Vincent (1970). The radiation data from 40N to 00N in July come from Katayama (1967); from the equator to 30S his N. Hemisphere data for January are substituted.

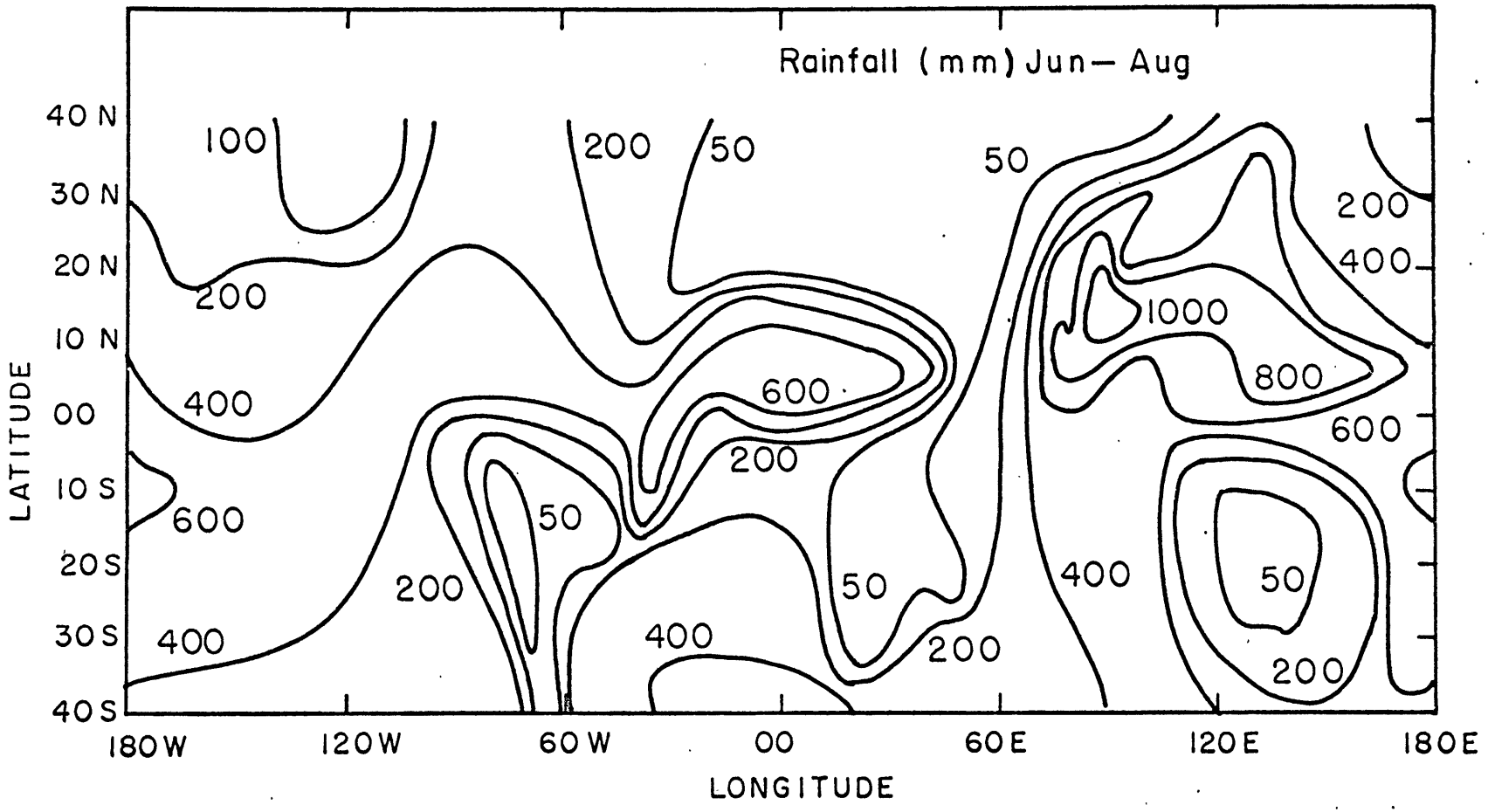

Figure 4.1 Mean precipitation for June-August in mm.

Boundary layer heating is confined mainly to the lower troposphere. The boundary layer heating can be neglected if the region of study is at 500 mb. The magnitude of each differential term is calculated freom observational data and its relative importance is evident from Table (4. 1).

Table (4. 1) shows that the vertical motion is controlled mainly by latent heat release and radiational cooling; the local change of temperature and the horizontal advection terms are two orders of magnitude smaller than the diabatic term. The local change of temperature is even smaller than the horizontal advection term. Davis (1963) has pointed out this, he said 'On the scale of the derived thermal budget, the rates of enthalpy storage were found to be of secondary importance.'

From Table (4. 1), it is realized that the first law of thermodynamis is not a good method to calculate of $\overline{\omega}$ because its value mainly depends on the small difference of two large quantities. Even a small error in the estimate of latent heat release and radiational cooling will introduce a large error in $\overline{\omega}$. The other problems are the estimation of the vertical distribution of latent heat release and the computation of solar heating and infrared cooling in the presence of clouds. With Katayama's (1967) radiational data, the $\overline{\omega}$-pattern calculated from equation (4. 2) is given at Figure (4. 2).

Table 4.1 Zonal Average of the First Law of Thermodynamics at 500 mb. unit: K/sec.

latitude	$\frac{\partial \bar{T}}{\partial t}$	$\bar{u}\frac{\partial \bar{T}}{\partial x}$	$\bar{v}\frac{\partial \bar{T}}{\partial y}$	latent heat release	net radiation cooling
35N	4.1×10^{-7}	1.1×10^{-7}	3.8×10^{-7}	1.1×10^{-5}	-1.7×10^{-5}
25N	2.0×10^{-7}	0.5×10^{-7}	0.0×10^{-7}	1.9×10^{-5}	-1.5×10^{-5}
15N	0.3×10^{-7}	0.7×10^{-7}	-1.3×10^{-7}	2.8×10^{-5}	-1.5×10^{-5}
05N	-0.6×10^{-7}	0.6×10^{-7}	0.9×10^{-7}	2.8×10^{-5}	-1.8×10^{-5}
05S	-0.4×10^{-7}	-0.2×10^{-7}	-0.7×10^{-7}	1.9×10^{-5}	-1.7×10^{-5}
15S	-0.1×10^{-7}	-0.2×10^{-7}	-9.0×10^{-7}	1.4×10^{-5}	-2.0×10^{-5}
25S	-1.0×10^{-7}	-0.7×10^{-7}	-26.6×10^{-7}	1.6×10^{-5}	-1.9×10^{-5}
35S	-3.0×10^{-7}	-6.8×10^{-7}	-9.5×10^{-7}	1.9×10^{-5}	-1.9×10^{-5}

There are three areas which show large rising motion: over the monsoon region, over central west Africa and over the central west Atlantic ocean. The general features of $\bar{\omega}$ obtained from the first law of thermodynamics are the same as those for $\bar{\omega}$ derived from the continuity equation. In general the magnitude of the peak rising motion is smaller than that obtained from the continuity equation. Between 5S and 25S the thermodynamic equation computation does not show general downward motion because in this latitude zone only a few stations are available. At these few stations the precipitation

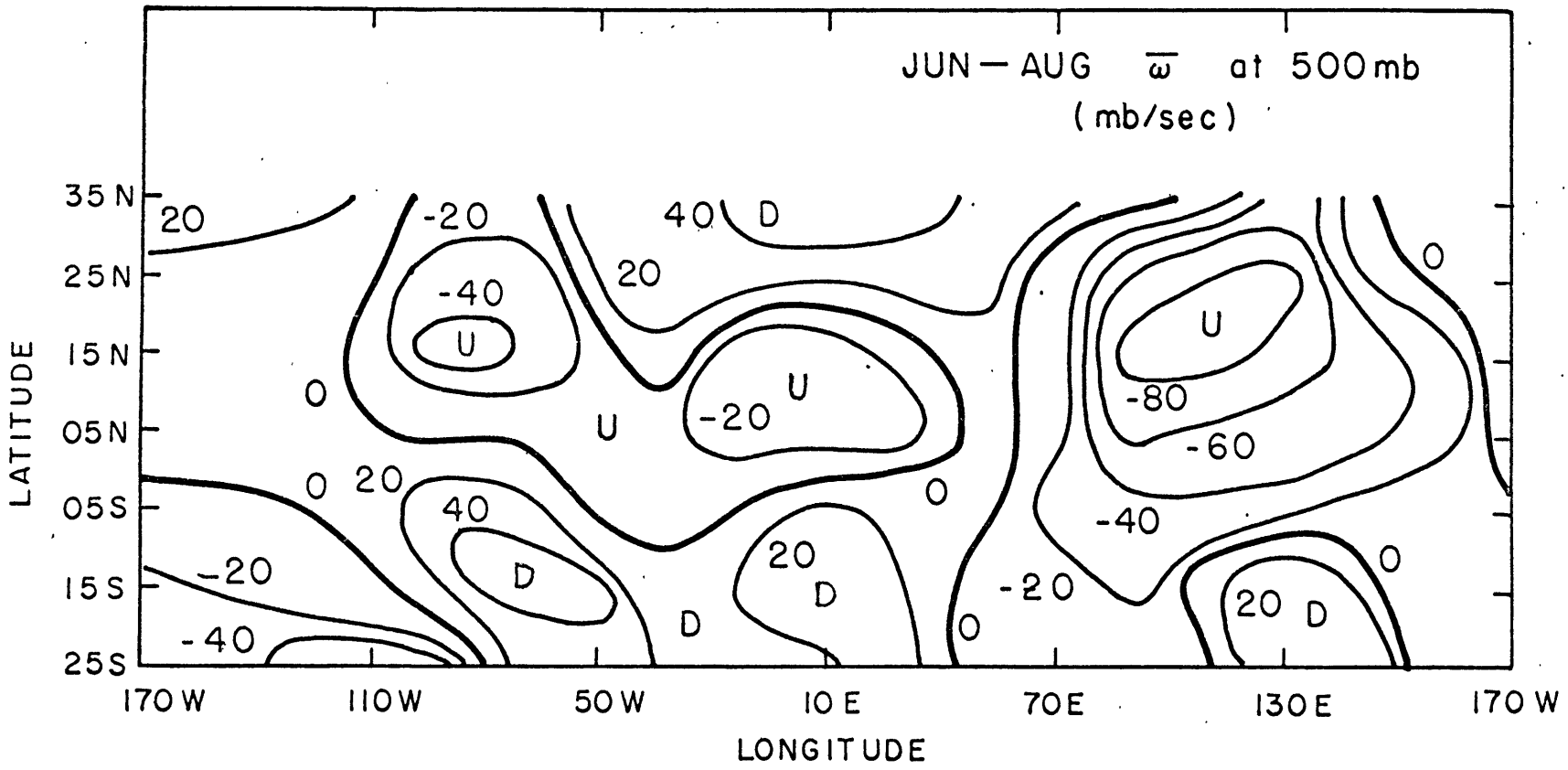

Figure 4.2 $\overline{\omega}$ at 500mb calculated from 1st law of thermodynamics in June-August

is large and is influenced by local topographic relief. These values cannot represent the precipitation over a vast ocean area. It is believed that the precipitation and the latent heat release are therefore overestimated in this region. This effect brings about motion in the southern Hadley cell region upward when vertical motions are calculated from the first law of thermodynamics in June-August. If $\overline{\omega}$ is obtained from the continuity equation, the vertical motion shows general downwards motion in the same region.

4.2 Calculated From the Continuity Equation

The continuity equation

$$\frac{\partial \overline{\omega}}{\partial p} = \frac{\partial \overline{u}}{\partial x} + \frac{\partial \overline{v}}{\partial y} \qquad (4.3)$$

is used for the evaluation of $\overline{\omega}$ where $\overline{u}$ and $\overline{v}$ are derived from observations. A correction to $\overline{v}$ is applied to ensure that there is no net mass flow across any latitude circle. This is $\int_{1000}^{100mb} [\overline{v}]\, dp = 0$ It is assumed that $\overline{\omega}$ =0 at 1000 mb and from equation (4.3) we can get $\overline{\omega}$ at every level from 850 mb to 100 mb. However due to the accumulation of error in the computation of divergence during the vertical integration of the continuity equation, $\overline{\omega}$ may deviate from zero at the top of the atmosphere if we integrate upwards from the lower boundary. For this reason $\overline{\omega}$ is set equal to zero at 100 mb and its value at each lower level is reduced by a factor varying linearly with pressure.

$\overline{\omega}$ computed from the continuity equation at 500 mb is given in Figure (4. 3). In June-August there are three regions which show large rising motion: over the monsoon region, over central west Africa and over ITCZ in the Pacific ocean. They may be compared with cloudiness value mapped by Hubert et al (1969). As mentioned previously the diabatic process is the predominant factor of control over the vertical motion of the atmosphere. All these regions with large upward motion coincide with the regions of large precipitation. The important of latent heat release in the tropics was also noted by Manabe and Smagorinsky (1967). They concluded that the condensation process markedly increased the intensity of the Hadley cell circulation. In the last chapter it was shown that in the monsoon region the condensation process also generates the Walker circulation. Latent heat release plays such an important role in the tropics that it is believed that the adiabatic method cannot be used to evaluate $\overline{\omega}$ in the tropics. $\overline{\omega}$ computed from the continuity equation gives downward motion in most of the region from 5S to 30S which is the sinking motion of the Hadley circulation. The zonal average of $\overline{\omega}$ is given in Figure (4. 4), the maximum upward motion is located at 5N between 400 mb and 500mb and is nearly zero at 5S. There is considerable longitudinal asymmetry in $\overline{\omega}$ along each latitude circle: for example at 10N the monsoon circulation causes

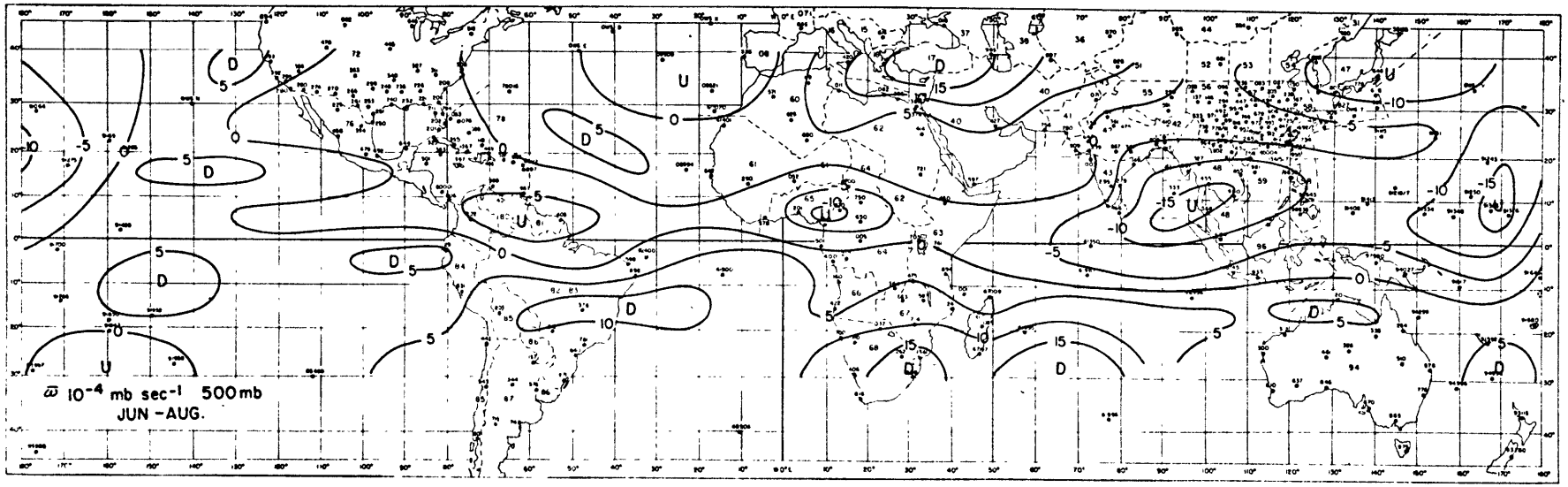

Figere 4.3 $\bar{\omega}$ calculated from the continuity equation for June-August at 500 mb, after Kyle (1970).

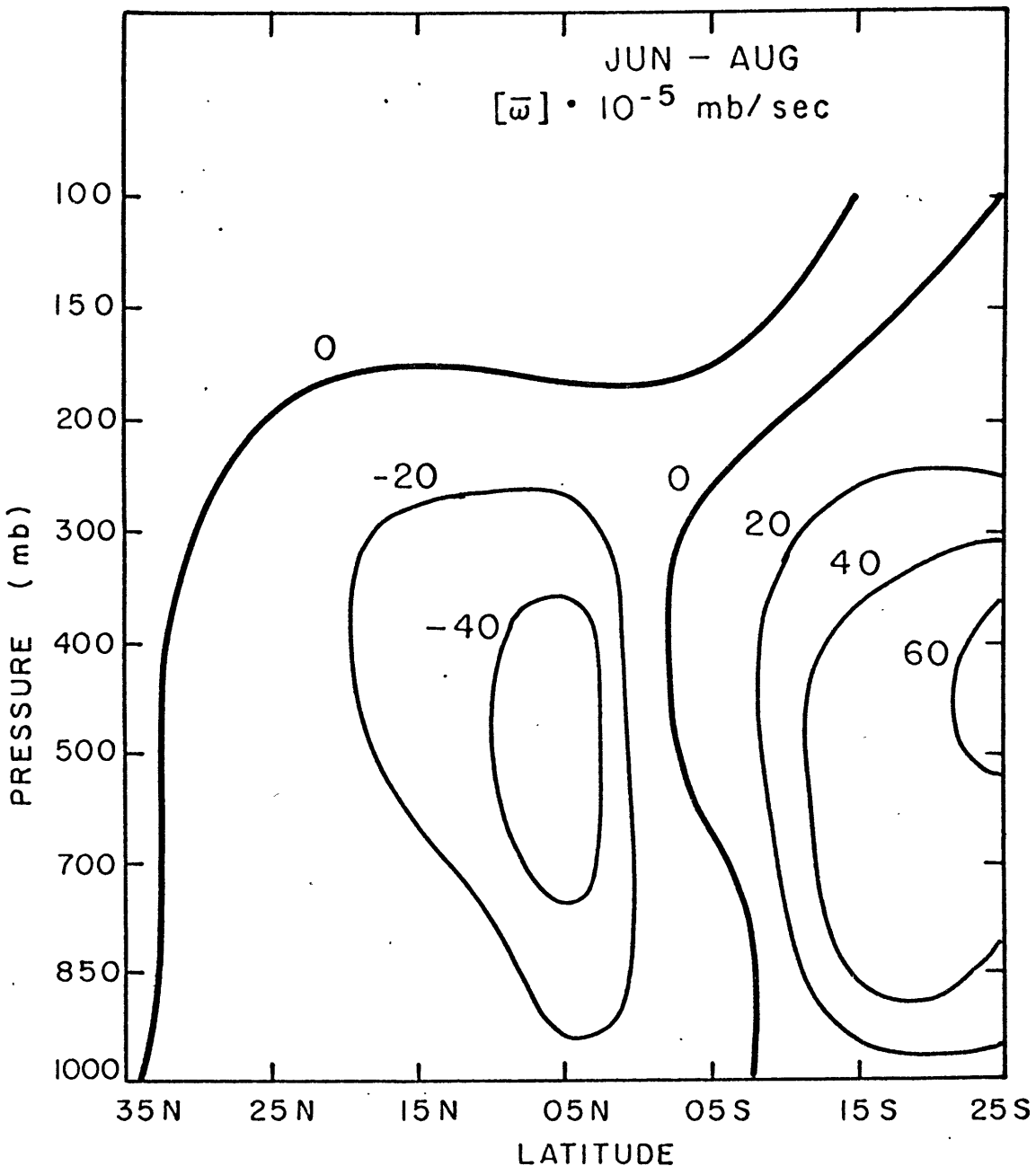

Figure 4.4 Zonal average of $\overline{\omega}$ for June-August

strong upward motion over India with $\overline{\omega}$ reaching the value of 160×10^{-5} mb/sec at 90E while values are close to zero over NE Pacific ocean. The vertical motion become downward along all latitude circle at 15S. The maximum downward motion in the tropical region is located at 25S. The zonal average flow pattern is presented in Figure (4. 5) where $[\overline{w}]$ is calculated from $\overline{w} \sim \frac{-\overline{\omega}}{\overline{\rho} g}$ The value of $[\overline{w}]$ is amplified by the factor of M in Figure (4. 5) which is equal to the ratio of the horizontal scale to the vertical scale as in Figure (4. 5). The length of the arrow indicates the magnitude which is equal to $\sqrt{M^2[\overline{w}]^2 + [\overline{v}]^2}$ and its direction is determined by $\tan^{-1} \frac{M[\overline{w}]}{[\overline{v}]}$. The $[\overline{w}]$ calculated from the continuity equation also guarantees that the streamlines in Figure (4. 5) is the same as the streamlines derived from the zonal average of mass flux presented in Figure (4. 6). They both show that the center of the Hadley cell is at 5N with a week Ferrel cell in the summer hemisphere.

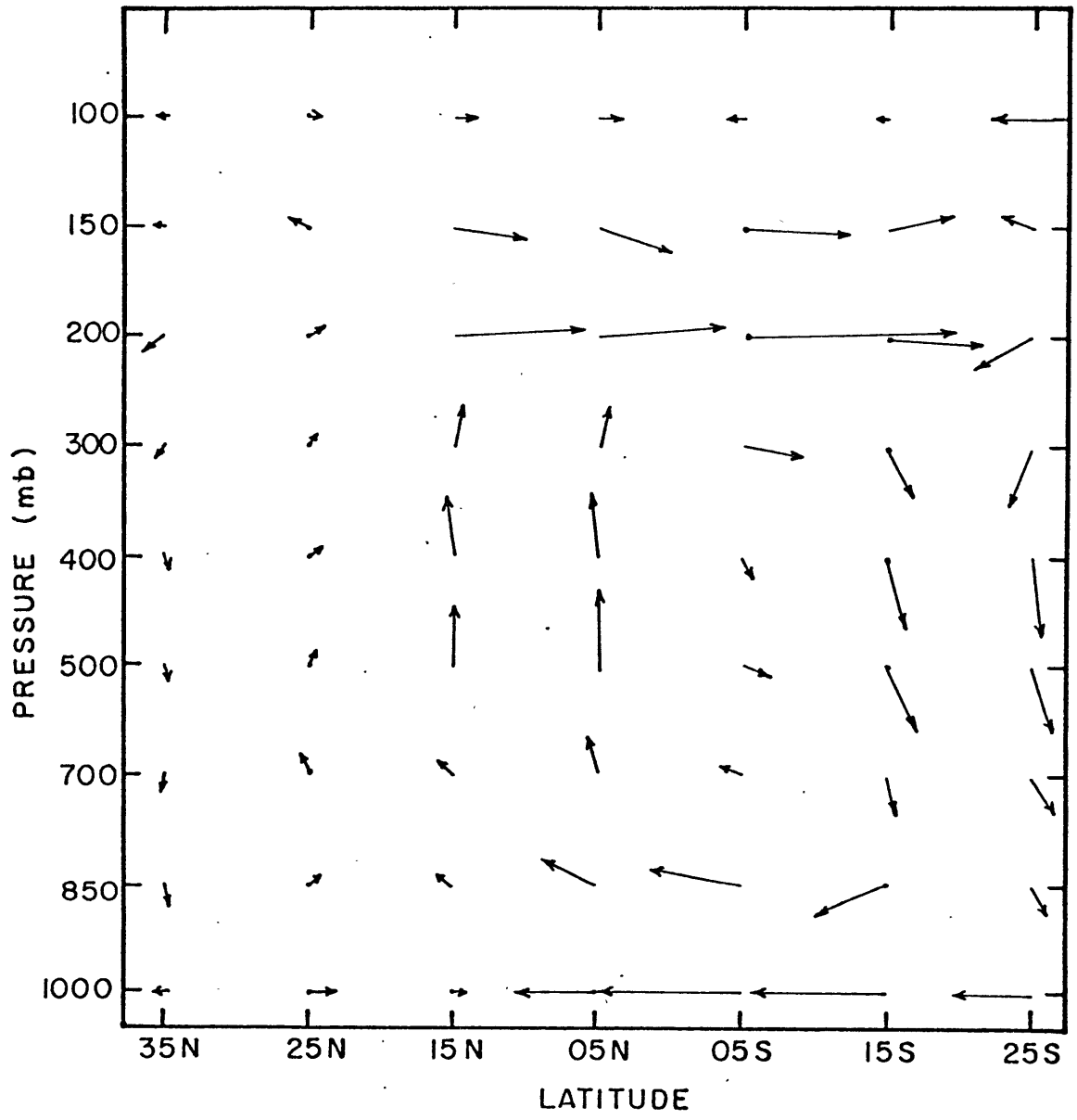

Figure 4.5 The direction of the streamlines of the mean meridional circulation at each grid point for June-August

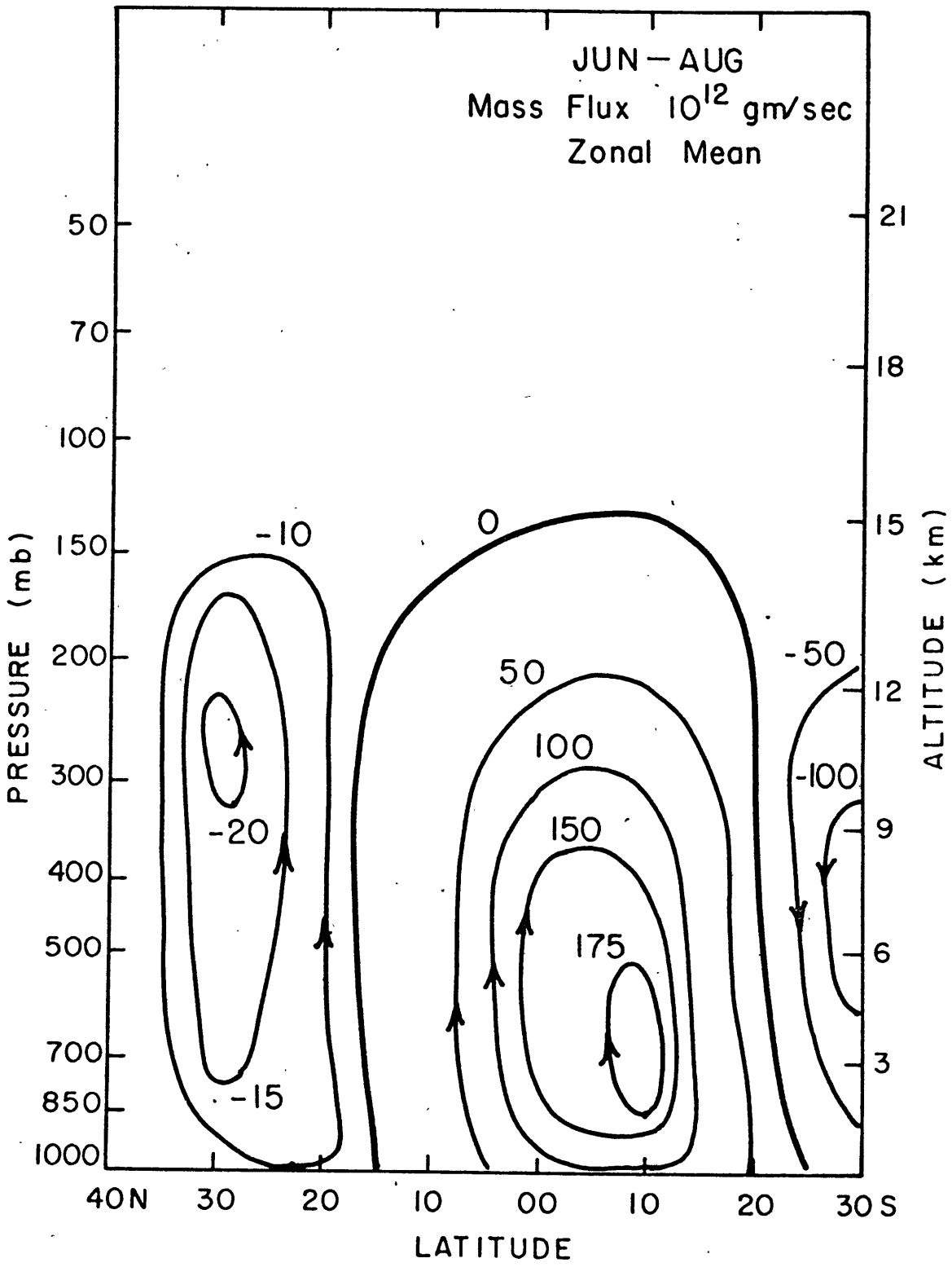

Figure 4.6 Streamlines of the mean meridional circulation as derived from mass flux for June-August

CHAPTER 5

LONGITUDINAL VARIATION OF ANGULAR MOMENTUM TRANSPORT

5.1 Horizonal Transport of Angular Momentum

The time-averaged total flux of angular momentum across a latitude circle may be written as

$$\frac{2\pi R^2 \cos^2\phi}{g} \int [\Omega R \cos\phi \, \bar{v} + \overline{uv}] \, d\phi \qquad (5.1)$$

The transport of Ω-angular momentum is zero because we assume no net mass flux across any latitude circle. The second term in the integrand may be further resolved into

$$[\overline{uv}] = [\bar{u}][\bar{v}] + [\bar{u}^* \bar{v}^*] + [\overline{u'v'}] \qquad (5.2)$$

where a bar denotes a time mean and brackets a zonal mean. Deviations from these means are indicated by a prime and an asterisk respectively. The terms on the RHS represent in order the mean meridional motion, the standing eddies and the transient eddies. The Ω-angular momentum transport for June-August is given in Table (5.1). The relative angular momentum transport is presented in Table (5.2) to (5.5). These are similar to the result by Kidson (1968) except that his values are given at 41N, 33N, 24N, 15N, 5N, 5S, 15S, 24S and 33S, whereas here the results are given at 40N,

The angular momentum transport (m^2/sec^2) and vertical integrals (10^{25} gm cm^2/sec^2) in June-August

Table 5.1 Ω -angular momentum

p(mb)	40N	30N	20N	10N	00N	10S	20S	30S
50	30.5	16.7	-124.9	-101.0	-12.9	26.5	-8.5	5.9
70	340.9	322.9	112.7	5.8	95.5	232.4	204.9	66.3
100	-113.8	99.4	132.1	244.7	87.8	-143.8	44.8	323.3
150	30.5	300.5	229.1	-327.1	-815.4	-830.0	-173.4	546.8
200	-11.1	-90.6	23.0	-619.4	-1512.2	-1300.1	-161.3	982.6
300	-5.1	10.0	-37.6	257.4	-415.4	-372.5	20.6	211.5
400	0.9	-34.7	-86.1	41.4	62.0	-118.4	-112.8	-112.5
500	-34.7	10.0	-49.8	3.2	-54.2	-296.3	-173.4	-224.3
700	12.7	-23.5	120.0	-22.2	165.2	84.9	-161.3	-213.1
850	-54.5	-112.9	10.9	92.2	655.5	949.0	178.2	-447.7
1000	87.9	21.2	-304.4	181.1	862.0	999.9	675.3	166.8
Integral	0.0	0.0	0.0	0.0	0.0	0.0	0.0	0.0

Table 5.2 Mean motion

p(mb)	40N	30N	20N	10N	00N	10S	20S	30S
50	-0.5	-0.5	4.8	2.7	0.1	0.0	-0.0	0.1
70	-0.4	-5.8	-3.3	-0.1	-0.3	0.4	1.9	1.5
100	-2.8	-0.3	-3.3	-6.0	-0.9	-0.3	1.1	14.7
150	1.3	3.1	-2.5	6.7	10.1	-8.1	-7.9	38.9
200	-0.6	-1.5	-0.1	10.4	26.9	-9.0	-8.1	76.7
300	-0.2	0.1	0.1	-3.0	6.2	-1.4	1.0	15.2
400	0.0	-0.3	0.5	-0.4	-0.8	0.3	-3.5	-6.0
500	-0.8	0.1	0.4	-0.0	0.6	1.8	-3.5	-8.5
700	0.2	-0.1	-0.7	0.2	-1.0	-0.4	-0.8	-3.7
850	-0.4	-0.0	-0.0	-0.3	-2.9	-8.2	-0.8	-3.2
1000	0.2	-0.0	1.1	-0.4	-2.9	-5.5	-2.4	0.1
Integral	-0.5	-0.3	-0.6	1.3	5.9	-6.7	-5.2	15.4

Table 5.3 Standing eddies

p(mb)	40N	30N	20N	10N	00N	10S	20S	30S
50	-0.3	0.6	1.0	1.1	-0.2	-0.3	-0.3	-0.1
70	1.0	1.4	1.3	0.9	0.3	1.0	1.0	-0.0
100	1.8	11.8	6.2	6.2	2.9	0.4	1.6	0.0
150	1.0	10.0	-0.5	6.5	17.9	22.6	10.5	0.2
200	2.1	11.9	3.3	3.9	10.1	11.3	8.2	-0.4
300	-0.4	3.8	2.3	1.9	1.6	1.3	0.3	1.7
400	-0.4	-0.3	0.5	0.1	-0.0	-0.3	-0.4	1.3
500	0.2	-0.5	1.6	-0.6	-0.7	0.2	-0.9	1.4
700	0.3	-0.5	-0.1	-0.6	0.1	-0.2	-0.9	2.2
850	1.7	-1.6	-4.3	-3.7	0.3	-0.7	-1.1	0.9
1000	-1.1	-0.5	2.2	3.5	-0.2	-0.2	0.1	0.1
Intergal	0.9	4.1	1.3	1.6	4.9	5.1	1.9	2.3

Table 5.4 Transient eddies

p(mb)	40N	30N	20N	10N	00N	10S	20S	30S
50	0.0	0.0	0.0	0.0	0.0	0.0	0.0	0.0
70	0.0	0.0	0.0	0.0	0.0	0.0	0.0	0.0
100	4.7	0.6	-1.9	-0.4	1.3	0.5	-3.4	-7.7
150	21.2	14.0	6.9	6.8	9.7	5.2	-13.2	-20.4
200	30.8	20.1	9.6	3.8	8.9	5.8	-12.9	-30.0
300	25.6	14.4	5.8	2.9	2.8	-1.3	-20.9	-45.3
400	10.3	7.4	3.3	1.6	-0.7	-3.7	-14.6	-27.9
500	6.9	4.8	3.0	1.1	-1.2	-3.6	-10.4	-19.8
700	2.3	2.5	2.6	1.2	-1.5	-4.1	-7.2	-10.1
850	-0.5	1.5	1.3	1.1	-1.0	-3.2	-4.1	-5.3
1000	0.3	0.9	0.8	0.6	-0.3	-1.1	-1.0	-0.0
Integral	17.0	13.2	7.5	4.2	2.0	-4.1	-21.6	-37.0

Table 5.5 Relative angular momentum

p(mb)	40N	30N	20N	10N	00N	10S	20S	30S
50	-0.9	0.1	5.9	3.7	-0.1	-0.2	-0.4	-0.1
70	0.6	-4.3	-2.1	0.7	0.0	1.4	2.9	1.5
100	3.8	12.2	1.0	-0.2	3.3	0.7	-0.7	7.0
150	23.6	27.1	3.8	20.1	37.7	19.7	-10.5	18.7
200	32.3	30.5	12.8	18.1	46.0	8.1	-12.8	46.4
300	25.0	18.3	8.3	1.7	10.6	-1.4	-19.7	-28.4
400	9.9	6.8	4.2	1.2	-1.5	-3.7	-18.6	-32.7
500	6.3	4.4	4.9	0.4	-1.3	-1.6	-14.8	-26.9
700	2.8	1.9	1.7	0.8	-2.4	-4.6	- 8.9	-11.6
850	0.8	-0.1	-3.1	-2.9	-3.6	-12.0	- 5.9	- 7.6
1000	-0.6	0.4	4.1	3.8	-3.5	-6.8	- 3.2	0.2
Integral	17.5	17.0	8.1	7.1	12.8	-5.6	-24.9	-19.3

30N, 20N, 10N, 00N, 10S, 20S and 30S. The Ω -angular momentum at each pressure level is much larger than the relative angular momentum though the vertical integral of the former is zero along the latitude circle. In the Hadley cell circulation there is northward transport of Ω -angular momentum in the low troposphere changing to southward transport in the upper troposphere. The results of the relative angular momentum transport are the same as those of Kidson (1968) and will not be repeated here.

The vertical integral of the total flux of angular momentum per unit length in longtitude at each grid point is written as

$$\frac{R\cos\phi}{g}\int_{50}^{1000\,mb}\left(\Omega R\cos\phi\,\bar{v}+\bar{u}\,\bar{v}+\overline{u'v'}\right)dp \qquad (5.3)$$

where the first term in the integrand represents the Ω -angular momentum by the net mass flux, the second term is the mean meridional transport of relative angular momentum and the third term is the transport by transient eddies. Vertical integrals of these components of the angular momentum transport are given in Tables (5.6), (5.7) and (5.8) respectively. The total relative angular momentum transport is given in Table (5.9). The Ω -angular momentum transport is about one or two orders of magnitude larger than the transport of relative angular momentum although

The vertical integral of the angular momentum transport (10^{16} gm cm/sec^2) per unit length in longitude in June-August

Table 5.6 Ω -angular momentum

Lat.	180W	160	140	120	100	80	60	40	20	00	20	40	60	80	100	120	140	160E
40N	183	126	-171	409	27	-158	116	3	-190	35	-350	259	-249	84	-156	-37	117	-50
30N	-68	-41	63	624	54	-6	99	-133	-133	437	-204	-66	-448	-95	-248	74	110	-17
20N	-119	106	162	149	-62	-51	196	16	78	107	34	-111	-376	-150	-141	124	78	-42
10N	4	126	193	136	33	-54	112	201	6	-110	5	46	-42	-392	-223	-63	-37	61
00N	66	12	-49	-10	-40	-48	160	132	-64	-84	52	380	136	-437	-196	-42	-13	45
10S	48	37	-93	-132	-139	-99	188	163	10	-66	55	295	145	-160	-252	6	86	-92
20S	-136	121	-80	-129	-186	16	77	117	20	-71	-117	-93	55	55	31	112	577	-145
30S	-46	96	-43	-173	-206	-283	52	69	5	-131	-222	-133	-53	202	220	222	427	-4

Table 5.7 mean motion

40N	1.6	2.5	-1.0	12.5	-0.8	-5.4	1.4	-0.3	-3.1	2.5	-5.4	13.1	-4.7	2.3	-7.2	-2.4	1.9	-4.6
30N	-2.1	1.3	6.4	5.0	-1.9	-0.7	-0.1	-0.3	1.1	4.8	2.2	1.4	-3.2	0.0	0.9	2.5	1.1	-1.0
20N	-0.5	3.9	1.9	0.8	0.0	-0.8	-1.6	0.4	-1.2	-0.8	-1.9	-6.9	-6.8	3.6	9.5	4.0	1.5	-0.6
10N	0.3	-0.6	-1.5	-1.4	-1.2	-0.5	-2.5	-2.5	0.2	2.4	0.3	-2.9	-0.6	3.5	12.6	5.7	1.8	-0.9
00N	-0.4	-0.7	0.8	0.7	1.1	0.4	-2.5	-2.8	1.0	3.9	2.5	0.8	8.3	14.2	14.5	4.5	1.2	-0.5
10S	0.8	1.1	-1.0	-1.2	-0.5	0.1	-0.6	-4.6	-4.8	-2.4	-1.5	-0.7	0.7	5.4	3.0	-0.3	-1.1	0.0
20S	-2.1	10.8	-1.5	-5.0	-6.0	-4.5	4.9	4.3	-1.1	-2.6	-1.5	-7.0	-12.2	-3.9	-2.2	6.5	17.3	-8.4
30S	-1.2	10.4	1.9	-4.3	-4.5	-3.1	14.9	11.3	4.2	-0.4	-3.7	-1.0	-3.0	8.1	12.2	21.3	31.7	-4.4

Table 5.8 transient eddies

Lat.	180W	160	140	120	100	80	60	40	20	00	20	40	60	80	100	120	140	160E
40N	4.2	5.4	5.6	3.3	2.3	5.4	5.3	3.4	4.2	4.2	6.6	4.8	2.5	0.9	1.7	4.1	7.7	4.4
30N	3.5	5.7	5.3	3.3	1.6	4.1	3.7	2.2	3.2	3.7	5.1	1.8	0.3	1.6	0.6	1.3	5.0	3.9
20N	1.8	3.4	3.6	1.0	-0.6	2.0	1.8	1.8	1.8	1.6	1.6	-0,3	1.2	0.4	1.4	3.3	4.2	3.6
10N	0.9	1.7	1.6	0.5	0.1	0.6	-0.1	1.6	1.5	1.1	0.6	-0.5	0.3	2.1	0.7	3.5	2.0	1.0
00N	-0.4	0.8	0.6	0.1	0.3	0.2	-0.8	0.9	1.5	1.7	0.4	-1.0	0.2	1.1	0.9	1.8	0.7	0.0
10S	-2.2	-0.8	-0.5	-0.7	-1.6	-1.3	-1.6	-0.6	-0.4	-0.2	-0.5	-2.0	-1.3	-0.8	-1.2	-1.3	-1.6	-1.0
20S	-5.2	-4.8	-3.2	-4.0	-6.5	-10.0	-7.2	-5.4	-4.7	-6.7	-4.4	-3.0	-3.7	-4.8	-6.9	-6.5	-6.6	-3.1
30S	-6.3	-7.0	-7.7	-8.9	-10.9	-12.9	-9.3	-7.8	-8.6	-12.1	-11.6	-8.8	-8.8	-9.5	-11.8	-11.1	-7.4	-5.0

Table 5.9 relative angular momentum

40N	5.8	7.9	4.6	15.8	1.5	0.0	6.7	2.6	1.1	6.8	1.2	18.0	-2.3	3.2	-5.4	1.7	9.6	-0.2
30N	1.4	6.9	11.6	8.3	-0.3	3.4	3.6	0.9	4.3	9.9	4.1	1.7	-1.6	0.6	2.2	7.5	8.3	2.8
20N	1.3	7.3	5.4	0.2	-0.3	1.2	0.2	2.2	0.6	0.8	-0.4	-6.8	-5.6	4.0	10.9	7.4	5.7	3.0
10N	1.2	1.1	0.1	-0.9	-1.1	0.1	-2.6	-0.9	1.7	3.5	0.9	-3.3	-0.4	5.6	13.3	9.2	3.7	0.1
00N	-0.8	0.1	1.4	0.8	1.4	0.6	-3.3	-1.8	2.5	5.6	2.9	-0.2	8.5	15.3	15.4	6.3	1.9	-0.5
10S	-1.3	0.3	-1.6	-1.8	-2.1	-1.3	-2.2	-5.2	-5.2	-2.2	-1.0	-2.8	-0.7	4.6	1.8	-1.6	-2.8	-1.0
20S	-7.3	6.1	-4.7	-9.0	-12.4	-14.6	-2.3	-1.1	-5.8	-9.0	-5.9	-10.0	-15.9	-8.7	-9.2	-0.0	10.7	-11.7
30S	-7.5	3.4	-5.9	-13.2	-15.5	-16.0	5.6	3.4	-4.4	-12.5	-15.3	-9.8	-11.7	-1.4	0.4	10.1	24.3	-9.4

It is zero for the zonal average for the whole depth of the atmosphere, it is very important for any limited region in the tropics. Ananthakrishnan et al (1967) found that the Ω-transport term is one or two orders of magnitude large than the other meridional transport terms in the monsoon region. Keshavamurty (1968) studied the budget of angular momentum over the Indian monsoon region and also concluded that the Ω-transport term is the dominant term.

The total angular momentum transport across the equator into the summer hemisphere is 12.8×10^{25} gm cm^2/sec^2. From Table (5.8) the transient eddies bring about transport northward everywhere into the summer hemisphere at the equator except over small regions 40E, 60W and 180W. The exchange of atmospheric angular momentum between the hemispheres has been discussed by Kidson and Newell (1969). There is a strong southward transport of Ω-angular momentum over the monsoon region and a slightly weaker southward transport over Eastern North America. This may due to the deflection of the uniform zonal current by the Himalaya mountains and the Rocky mountains respectively as was discussed in chapter 3. There is a large northward transport of angular momentum by mean motion over the monsoon region. In the upper troposphere, the wind generally shows NE direction in this region. Both $\bar{u}$ and $\bar{v}$ are negative, their product gives a large northward transport of angular momentum. It is inter-

esting to note from Table (5.8) that the transport by transient eddies is northward in the Northern Hemisphere and southward in the Southern Hemisphere. The reason the zonal average of the transient eddy transport is the dominant term in the total angular momentum transport is that the values at different longitudes reinforce each other.

5.2 Vertical Transport of Angular Momentum

It is known that in the tropics there is generally an easterly wind at the surface and thus in this region a continuous flow of absolute angular momentum from the earth to the atmosphere. At middle latitudes there is generally a westerly wind at the surface and hence a continuous flow of absolute angular momentum from the atmosphere to the earth. Starr (1951) has pointed out that the horizontal transport is mainly due to eddy processes and that there is a maximum transport at 200 mb. By what process is the angular momentum transport upward? The answer to this question depends on the vertical velocity within the atmosphere. The vertical motion is obtained from the continuity equation. The vertical transport of angular momentum across a pressure level may be written as

$$\frac{R^3 \cos^2\phi}{g} \int_{\phi_1}^{\phi_2} \int_{\lambda_1}^{\lambda_2} \left(\Omega R \cos\phi\, \bar{\omega} + \bar{u}\,\bar{\omega} + \overline{u'\omega'}\right) d\lambda\, d\phi \qquad (5.4)$$

Here $d\lambda$ was taken as 20 degrees, $d\phi$ on 10 degrees. The second term in the integrand may be resolved as before into the transport by mean motion, standing eddies and transient eddies. As vertical velocity was not computed on a daily basis the transient eddies transport is omitted here. In the whole tropical region $u' \ll \bar{u}$, and even if $\omega' \sim \bar{\omega}$ the transport by the transient eddies is much smaller than that by the mean motion. The omission of transient eddies does not produce a large error. Results of the computation of zonal average vertical angular momentum transports are presented in Tables (5.10), (5.11) and (5.12).

From these tables the vertical transport is mainly contributed by Ω -angular momentum and in the tropical region the vertical transport is related to the Hadley cell circulation. The vertical transport of Ω -angular momentum is upwards from 25N to 5S and downwards at 35N and from 15S to 25S.

The vertical transport of relative angular momentum is about one or two orders magnitude smaller than that of Ω -angular momentum. The longitudinal asymmetry of the vertical transport

Vertical angular momentum transport in June-August in the tropical region

Table 5.10 Ω -angular momentum, unit: 10^{27} gm/cm^{2}sec^2

p(mb)	35N	25N	15N	05N	05S	15S	25S
150	0.00	0.00	0.11	0.20	0.05	-0.22	-0.17
200	0.20	-0.09	-0.16	-0.06	-0.08	0.08	0.20
300	0.33	-0.23	-1.59	-1.62	0.20	1.89	1.95
400	0.22	-0.28	-1.98	-3.37	0.61	3.43	3.16
500	0.12	-0.47	-1.33	-3.88	0.53	3.60	3.10
700	0.08	-0.77	-0.54	-3.17	-0.32	3.26	2.38
850	0.09	-0.56	-0.35	-2.22	-0.70	2.48	1.67

Table 5.11 Mean motion, unit: 10^{25} gm/cm^{2}sec^2

p(mb)	35N	25N	15N	05N	05S	15S	25S
150	0.01	0.00	-0.17	-0.32	-0.01	-0.60	-0.97
200	0.69	-0.05	0.18	0.11	0.05	0.23	1.28
300	0.91	-0.14	1.16	2.17	-0.11	4.67	11.43
400	0.44	-0.05	1.63	3.93	-0.46	4.80	13.23
500	0.18	0.03	1.20	4.18	-0.45	2.48	8.85
700	0.06	0.11	0.37	2.16	0.17	0.09	2.56
850	0.03	0.13	0.13	0.83	0.45	-1.61	0.20

Table 5.12 standing eddies, unit: 10^{25} gm/cm^2 sec^2

p(mb)	35N	25N	15N	05N	05S	15S	25S
150	-0.06	0.03	-0.27	0.20	0.21	0.05	-0.02
200	0.30	0.20	-0.06	0.44	0.36	0.12	-0.24
300	0.97	0.40	0.15	0.31	0.74	-0.18	-1.12
400	0.83	0.08	-0.38	-0.36	0.42	-0.36	-1.83
500	0.05	-0.13	-0.93	-0.79	-0.29	-0.41	-1.57
700	-0.24	-0.13	-0.75	-0.38	0.20	-0.12	-0.65
850	-0.15	-0.13	-0.41	-0.49	0.02	-0.01	-0.03

of Ω -angular momentum is the same as the longitudinal asymmetry of the $\overline{\omega}$ pattern. There are larger upward vertical transports over the monsoon region, over Nigeria and over the ITCZ in the Pacific ocean. The relative importance of the zonally averaged horizontal and vertical angular momentum transports for the whole atmospheric column is illustrated in Figure (5.1).

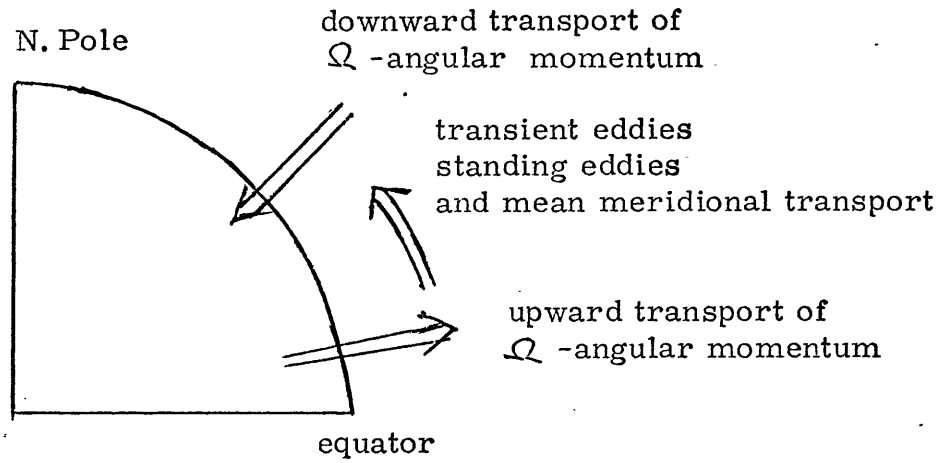

Fig. 5.1 The horizontal and the vertical transport of angular momentum in tropics

For the whole tropical atmosphere the Ω -angular momentum is the dominant term in the vertical transport. The transient eddies and mean meridional motion are important for its horizontal angular momentum transport. The standing eddies is also quite significant in equatorial regions.

CHAPTER 6

MEAN KINETIC ENERGY BUDGET IN THE TROPICAL REGION

Due to spatial variations of atmospheric heating produced by latent heat release and radiative processes, potential and internal energy are continuously created in the atmosphere and converted by air motions into kinetic energy which finally through the action of frictional dissipation turns into heat. In June-August the latent heat release creates the monsoon circulation which cause a large asymmetry in the tropics. The vertical integral of the mean kinetic energy is:

$$\frac{1}{g}\int_{50\,mb}^{1000\,mb}\frac{1}{2}(\bar{u}^2+\bar{v}^2)\,dp \qquad (6.1)$$

and is given in Figure (6. 1). The major feature is the large mean kinetic energy in the monsoon region (4.6×10^8 erg/cm^2) which is about four times larger than other regions at the same latitude. Why is the mean kinetic energy so large in the monsoon region and what's the force which maintains it? To answer this question, it is natural to look at the energy cycle. Unfortunately the complete energy cycle can be obtained only based on zonal averages and from this viewpoint the monsoon characteristics disappear. If we look at some limited region the energy transport across the boundary of

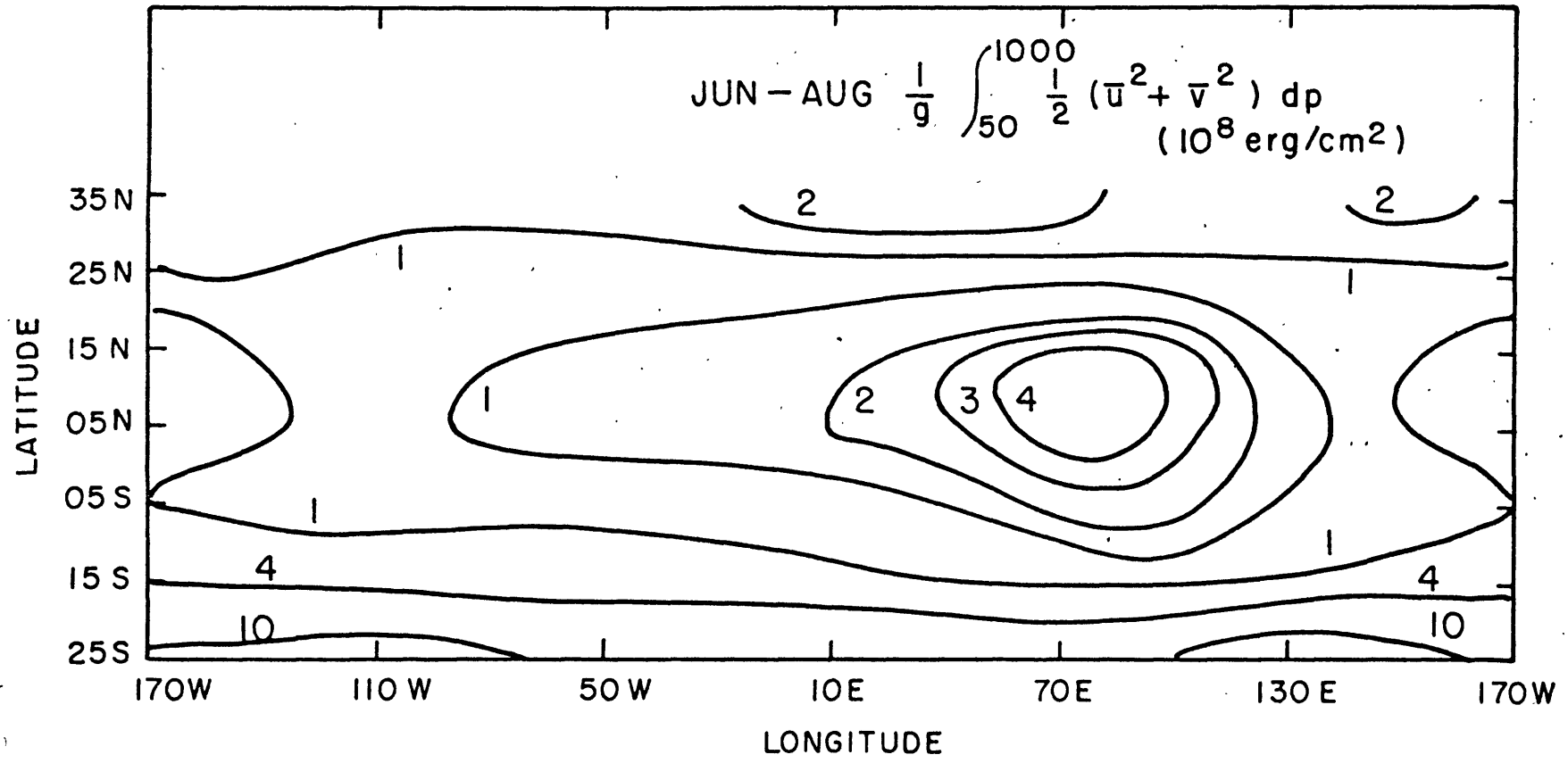

Figure 6.1 Vertical intergral of mean kinetic energy for June-August

the limited region is important (Smith 1969) and the energy conversion in the energy cycle loses its meaning. But computations of the terms in the energy cycle of a limited region are still valuable and may be compared with the results of zonal averages calculated by some other methods. The atmospheric energy cycle has been studied by Oort (1964) in the Northern Hemisphere and Vincent (1970) in the tropical regions, but the problem of kinetic energy dissipation in the tropical region is untouched. The dissipation of kinetic energy in various regions during various periods are given in Table (6. 1).

Kung (1969) estimated that the rate of frictional dissipation is about 4320 ergs/cm^{2}sec over North America. Is this value the same in the tropics? What is the percentage due to mean kinetic energy dissipation and that due to eddy kinetic energy dissipation? Oort (1964) and Dutton and Johnson (1967) indicate that the eddy kinetic energy dissipation is about ten times larger than the mean kinetic energy dissipation in the Northern Hemisphere.

6. 1 Equations

The equation used for the calculation of the mean kinetic energy dissipation is different from Holopainen (1963) and Kung (1966, 1969) who carried out computations on a daily basis. All the data used here averaged over a seven year period for each season.

Table 6.1 Frictional Dissipation by Various Investigators Unit: ergs/cm^{2}sec

Investigator	Thickness (mb)	Total KE dissip.	MKE dissip.	EKE dissip.	Region	Period
Holopainen (1963)	sfc-200	10400	----	----	England	Jan. 1954
Oort * (1964)	1000-100	2300	200	2100	Northern Hemisphere	one year
Kung (1966a)	sfc-100	6380	----	----	North America	Feb.-Aug. 1962; Jan. 1963
Kung (1966b)	sfc-50	7124	----	----	North America	11 months 1962-63
		8283	----	----		winter
		6817	----	----		spring
		6535	----	----		summer
		6863	----	----		autumn
Kung (1969)	sfc-50	4320	----	----	North America	annual
		3280	----	----		summer
		4320	----	----		winter
Dutton & Johnson (1967)**	1000-150	6400	550	5850	Northern Hemisphere	annual
Vincent (1970)*	1000-100	----	----	826	30N-30S	1957-64
		----	----	1190		winter
		----	----	695		spring
		----	----	740		summer
		----	----	680		autumn

* These values are derived from the diagrams of his energy cycles and not from direct calculation.

** His values relied on Kung's (1966a) estimate of total frictional dissipation.

If the atmosphere is assumed to be in a state of hydrostatic equilibrium, we may express the equations of motion and continuity in (x, y, p) coordinates as follows:

$$\frac{\partial u}{\partial t} + u\frac{\partial u}{\partial x} + v\frac{\partial u}{\partial y} + \omega\frac{\partial u}{\partial p} - fv = -g\frac{\partial z}{\partial x} + F_x \qquad (6.2)$$

$$\frac{\partial v}{\partial t} + u\frac{\partial v}{\partial x} + v\frac{\partial v}{\partial y} + \omega\frac{\partial v}{\partial p} + fu = -g\frac{\partial z}{\partial y} + F_y \qquad (6.3)$$

$$\frac{1}{\rho}\nabla_z p = g\nabla_p z \qquad (6.4)$$

$$\frac{\partial u}{\partial x} + \frac{\partial v}{\partial y} + \frac{\partial \omega}{\partial p} = 0 \qquad (6.5)$$

Equs. (6.2), (6.3) and (6.5) take averaging with respect to time and using the continuity equ. (6.5), the following equations are obtained

$$\frac{\partial \bar{u}}{\partial t} + \frac{\partial}{\partial x}(\overline{uu}) + \frac{\partial}{\partial y}(\overline{uv}) + \frac{\partial}{\partial p}(\overline{u\omega}) - f\bar{v} = -g\frac{\partial \bar{z}}{\partial x} + \bar{F}_x$$

$$\frac{\partial \bar{v}}{\partial t} + \frac{\partial}{\partial x}(\overline{uv}) + \frac{\partial}{\partial y}(\overline{vv}) + \frac{\partial}{\partial p}(\overline{v\omega}) + f\bar{u} = -g\frac{\partial \bar{z}}{\partial y} + \bar{F}_y$$

Equs. (6.6) and (6.7) multiplied by $\bar{u}$ and $\bar{v}$ respectively give:

$$\frac{\partial}{\partial t}\left(\frac{1}{2}\bar{u}^2\right)+\bar{u}\frac{\partial}{\partial x}(\overline{uu})+\bar{u}\frac{\partial}{\partial y}(\overline{uv})+\bar{u}\frac{\partial}{\partial p}(\overline{u\omega})-f\bar{u}\bar{v} = -g\bar{u}\frac{\partial\bar{z}}{\partial x}+\bar{u}\bar{F}_x \qquad (6.8)$$

$$\frac{\partial}{\partial t}\left(\frac{1}{2}\bar{v}^2\right)+\bar{v}\frac{\partial}{\partial x}(\overline{uv})+\bar{v}\frac{\partial}{\partial y}(\overline{vv})+\bar{v}\frac{\partial}{\partial p}(\overline{v\omega})+f\bar{u}\bar{v} = -g\bar{v}\frac{\partial\bar{z}}{\partial y}+\bar{v}\bar{F}_y \qquad (6.9)$$

Simplifying equs. (6.8) and (6.9) finally we get the following equations:

$$\frac{\partial}{\partial t}\left[\frac{1}{2}(\bar{u}^2+\bar{v}^2)\right]+\frac{\partial}{\partial x}\left[\bar{u}\frac{1}{2}(\bar{u}^2+\bar{v}^2)\right]+\bar{u}\frac{\partial\overline{u'u'}}{\partial x}+\bar{v}\frac{\partial\overline{u'v'}}{\partial x}$$
$$+\frac{\partial}{\partial y}\left[\bar{v}\frac{1}{2}(\bar{u}^2+\bar{v}^2)\right]+\bar{u}\frac{\partial\overline{u'v'}}{\partial y}+\bar{v}\frac{\partial\overline{v'v'}}{\partial y}$$
$$+\frac{\partial}{\partial p}\left[\bar{\omega}\frac{1}{2}(\bar{u}^2+\bar{v}^2)\right]+\bar{u}\frac{\partial\overline{u'\omega'}}{\partial p}+\bar{v}\frac{\partial\overline{v'\omega'}}{\partial p}$$
$$=-g\bar{u}\frac{\partial\bar{z}}{\partial x}-g\bar{v}\frac{\partial\bar{z}}{\partial y}+\bar{u}\bar{F}_x+\bar{v}\bar{F}_y \qquad (6.10)$$

Where $\bar{u}\,\bar{F}x + \bar{v}\,\bar{F}y$ is the mean kinetic energy dissipation and $-g\overline{\vec{V}\cdot\nabla z}$ depends on the ageostrophic component of the observed winds. The mean kinetic energy dissipation can be evaluated as a residual term in equation (6.10). The 9th and 10th terms in LHS of equation (6.10) is omitted because we did not have the covariance data between ω' and u', v'; and as mentioned previously it is believed that the covariance between ω' and

u' and v' is small. Equ. (6.10) written in finite difference from with the uncentered method gives:

$$\frac{\bar{K}^{n+1}_{i+\frac{1}{2},j+\frac{1}{2},k+\frac{1}{2}} - \bar{K}^{n-1}_{i+\frac{1}{2},j+\frac{1}{2},k+\frac{1}{2}}}{2\Delta t} + \frac{(\bar{u}\bar{K})^{n}_{i+1,j+\frac{1}{2},k+\frac{1}{2}} - (\bar{u}\bar{K})^{n}_{i,j+\frac{1}{2},k+\frac{1}{2}}}{\Delta x}$$

$$+ \bar{U}^{n}_{i+\frac{1}{2},j+\frac{1}{2},k+\frac{1}{2}} \frac{(\overline{u'u'})^{n}_{i+1,j+\frac{1}{2},k+\frac{1}{2}} - (\overline{u'u'})^{n}_{i,j+\frac{1}{2},k+\frac{1}{2}}}{\Delta x}$$

$$+ \bar{V}^{n}_{i+\frac{1}{2},j+\frac{1}{2},k+\frac{1}{2}} \frac{(\overline{u'v'})^{n}_{i+1,j+\frac{1}{2},k+\frac{1}{2}} - (\overline{u'v'})^{n}_{i,j+\frac{1}{2},k+\frac{1}{2}}}{\Delta x}$$

$$+ \frac{(\overline{v}\bar{K})^{n}_{i+\frac{1}{2},j+1,k+\frac{1}{2}} - (\bar{v}\bar{K})^{n}_{i+\frac{1}{2},j,k+\frac{1}{2}}}{\Delta y} + \bar{U}^{n}_{i+\frac{1}{2},j+\frac{1}{2},k+\frac{1}{2}} \frac{(\overline{u'v'})^{n}_{i+\frac{1}{2},j+1,k+\frac{1}{2}} - (\overline{u'v'})^{n}_{i+\frac{1}{2},j,k+\frac{1}{2}}}{\Delta y}$$

$$+ \bar{V}^{n}_{i+\frac{1}{2},j+\frac{1}{2},k+\frac{1}{2}} \frac{(\overline{v'v'})^{n}_{i+\frac{1}{2},j+1,k+\frac{1}{2}} - (\overline{v'v'})^{n}_{i+\frac{1}{2},j,k+\frac{1}{2}}}{\Delta y}$$

$$+ \bar{W}^{n}_{i+\frac{1}{2},j+\frac{1}{2},k+\frac{1}{2}} \frac{(\bar{w}\bar{K})^{n}_{i+\frac{1}{2},j+\frac{1}{2},k+1} - (\bar{w}\bar{K})^{n}_{i+\frac{1}{2},j+\frac{1}{2},k}}{\Delta p}$$

$$= -g\,\bar{u}^{n}_{i+\frac{1}{2},j+\frac{1}{2},k+\frac{1}{2}} \frac{\bar{z}^{n}_{i+1,j+\frac{1}{2},k+\frac{1}{2}} - \bar{z}^{n}_{i,j+1,k+\frac{1}{2}}}{\Delta x}$$

$$- g\,\bar{v}^{n}_{i+\frac{1}{2},j+\frac{1}{2},k+\frac{1}{2}} \frac{\bar{z}^{n}_{i+\frac{1}{2},j+1,k+\frac{1}{2}} - \bar{z}^{n}_{i+\frac{1}{2},j,k+\frac{1}{2}}}{\Delta y}$$

$$+ (\bar{u}\bar{F}_x)^{n}_{i+\frac{1}{2},j+\frac{1}{2},k+\frac{1}{2}} + (\bar{v}\bar{F}_y)^{n}_{i+\frac{1}{2},j+\frac{1}{2},k+\frac{1}{2}} \qquad (6.11)$$

where $\bar{K} = \frac{1}{2}(\bar{u}^2 + \bar{v}^2)$ hereafter define as the mean kinetic energy, the subscripts (i, j, k) are used to designate the independent variables (x, y, p) and the distances between two adjacent points in the x, y, p directions by Δx, Δy, Δp respectively which are not constant but depend on geographical latitude and pressure level. The superscript n refers to one season, n+1 refers to the next season, and n-1 refers to the preceding season. The subscripts (i + 1/2, j + 1/2, k + 1/2) are the smoothing values of adjacent grid points. For example,

$$U^{n}_{i+\frac{1}{2},j+\frac{1}{2}+k+\frac{1}{2}} = \Big(\bar{U}^{n}_{i\,j\,k} + \bar{U}^{n}_{i+1\,j\,k} + \bar{U}^{n}_{i\,j+1\,k} + \bar{U}^{n}_{i+1\,j+1\,k} + \bar{U}^{n}_{i\,j\,k+1} + \bar{U}^{n}_{i+1,j,k+1} + \bar{U}^{n}_{i\,j+1\,k+1} + \bar{U}^{n}_{i+1,j+1,k+1} \Big) \Big/ 8$$

All data are read at 18 grid points from 180W to 160E spaced 20 degrees apart in longitude, 8 grid points from 40N to 30S spaced 10 degrees apart in latutude and 9 pressure levels at 1000, 850, 700, 500, 400, 300, 200, 150 to 100 mb. $\bar{\omega}$ is calculated from the continuity equation

$$\frac{\partial \bar{\omega}}{\partial p} = -\left(\frac{\partial \bar{u}}{\partial x} + \frac{\partial \bar{v}}{\partial y} \right)$$

and assuming $\bar{\omega} = 0$ at 1000 mb and 100 mb. The results from 35N to 25S at each pressure level 850, 700, 500, 400, 300, 200 and 150 mb are from Chapter 4.

6.2 Vertical Distribution of Terms in the Mean Kinetic Energy Budget

In this section all quantity $\widetilde{X}$ is denoted the vertical integrals between two pressure levels p_1 and p_2 of $\overline{X}$ are given by

$$\widetilde{X} = \frac{1}{g}\int_{p_1}^{p_2} \overline{X}\, dp$$

The dimension of $\widetilde{X}$ should be multiplied by gm/cm^2 and the bracket means an average over some region A

$$\{\widetilde{X}\} = \frac{1}{A}\int_A \widetilde{X}\, dA$$

However, for the sake of simplicity, the notation of vertical integrals and the area mean will be omitted. The vertical integral of the whole atmospheric column (1000 mb to 100 mb) of the mean kinetic energy budget and the local change of the mean kinetic energy are given in Table (6.2).

In general, mean kinetic energy is large at middle latitude and small at equatorial region but for the reason of the asymmetry in the tropical region, there is a large mean kinetic energy in the monsoon region. Mean kinetic energy in the monsoon region is four times larger than in other regions at the same latitude as shown in Figure (6.1).

The local change of mean kinetic energy as calculate from seasonal means is given in Figure (6.2); roughly separated by the equator with decrease over the Northern Hemisphere over the

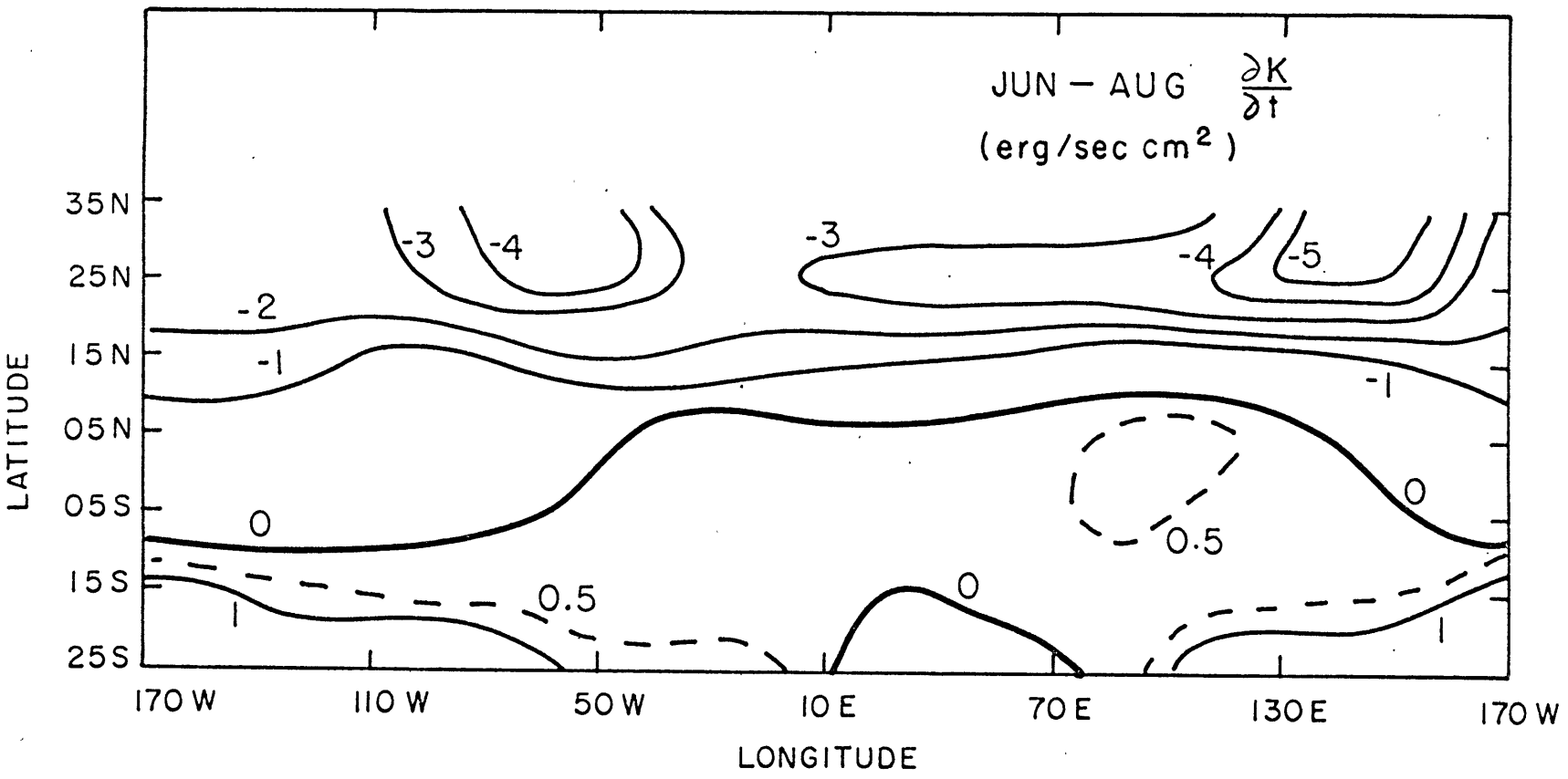

Figure 6.2 The vertical intergral of the local change of mean kinetic energy for June-August

period from March-May to September-November. The maximum rate of change in June-August is over the Pacific ocean east of Japan and over the NE Atlantic ocean. Maximum rates of change occur over these regions because Japan is influenced by the Mongolian high pressure center in winter and Aleutian high pressure center in summer while the NE Atlantic ocean is influenced by the Greenland high pressure center in winter and the North Central Atlantic high pressure center in summer. In these regions where two different high pressure systems successively influence the flow patterns, we expect to have a large local change of mean kinetic energy.

In the monsoon region, even though there are longitudinal asymmetry, for each quantities X the change with latitude $\partial X/\partial y$ is about one order magnitude larger then the change with longitude $\partial X/\partial x$. It is believed that in the tropics the horizontal scale lengths in the x and y directions are not equal. They are related roughly as follows:

$$\frac{\partial}{\partial x} \sim \frac{1}{L} \sim \frac{1}{10}\frac{\partial}{\partial y} \sim \frac{1}{10}\frac{1}{L/10}$$

where L is the longitudinal scale length which is about ten times larger than the scale length in the meridional direction. Table (6.3) is the same as Table (6.2) only some terms are combined and the physical meaning is much easier to observe from this table.

Table 6.2 Mean kinetic energy bedget within each pressure bounded layer in June-August in the tropical region (35N-25S) Unit: $erg/cm^2 sec$

Pressure layer (mb)	$\frac{\partial \bar{K}}{\partial t}$	$\frac{\partial}{\partial y}(\bar{v}\bar{K})$	$\frac{\partial}{\partial x}(\bar{u}\bar{K})$	$\bar{u}\frac{\partial \overline{u'u'}}{\partial x}$	$\bar{v}\frac{\partial \overline{u'v'}}{\partial x}$	$\bar{u}\frac{\partial \overline{u'v'}}{\partial y}$	$\bar{v}\frac{\partial \overline{v'v'}}{\partial y}$	$\frac{\partial}{\partial p}(\bar{\omega}\bar{K})$	$g\bar{u}\frac{\partial \bar{z}}{\partial x}$	$g\bar{v}\frac{\partial \bar{z}}{\partial y}$	$\bar{u}\bar{F}_x+\bar{v}\bar{F}_y$
100-150	-1.38	-21.9	0.0	0.2	0.2	9.2	0.0	-14.2	56.5	-64.7	-36.0
150-200	-1.91	-64.9	0.0	0.1	0.2	22.7	0.2	32.8	28.6	-20.0	-1.9
200-300	-2.58	-118.0	0.0	0.1	-0.3	62.1	0.4	158.0	28.5	70.7	199.0
300-400	-1.06	-28.3	0.0	0.0	0.1	38.9	0.2	-48.2	-15.1	0.4	-53.1
400-500	-0.55	-1.4	0.0	0.0	0.2	13.2	0.3	-79.8	-12.5	-59.9	-140.0
500-700	-0.46	-1.4	0.1	0.2	0.1	4.9	0.5	-52.5	-21.1	-73.2	-143.0
700-850	-0.09	-0.7	0.1	0.2	0.0	-1.4	0.0	1.8	-3.0	-23.7	-25.3
850-1000	-0.01	-0.1	0.0	0.1	0.1	-0.7	-0.5	2.1	-13.8	-171.0	-183.0

It is known that the center of the zonally averaged Hadley cell in June-August is located at 5N. Here the whole tropical region is divided into two, the North Hadley region (35N-05N) and the South Hadley region (05N-25S), the mean kinetic energy of these regions are presented in Table (6.4) and (6.5). The mean kinetic energy budget in the monsoon region (10E-170E, 25N-05N) is given in Table (6.6). From these tables, the horizontal pressure gradient force is the dominant term in the lower troposphere in every region. In the boundary layer all the dissipation of the mean kinetic energy is balanced by the horizontal pressure gradient force while the other parameters are negligibly small. Due to the large vertical velocity in the tropics the vertical transport of kinetic erergy is also important in the middle troposphere which is different from middle latitudes where the vertical transport is quite small (Kung 1966). In the upper troposphere the horizontal pressure gradient force is again generally the most important factor, but horizontal transport of mean kinetic energy , Reynolds stress transport and vertical transport are also quite important. The local change of mean kinetic energy is insignificant. It is interesting to note the difference between these four regions. The horizontal pressure gradient force is large in the lower and upper parts of the troposphere while it is quite weak in the middle troposphere in all regions. In the lower tro-

posphere the horizontal pressure gradient force balances all the mean kinetic energy dissipation for the four regions. The horizontal Reynolds stress transport is important in the South Hadley region (05N-25S) but is small in other regions.

In general, the vertical transport is important in the middle troposphere in the tropics. The horizontal transport of mean kinetic energy is of opposite sign between the North Hadley region and the South Hadley region. In the lower troposphere the horizontal pressure gradient force contribution is negative and in the upper troposphere it is positive in the North Hadley region; the reverse applies in the South Hadley region except in the boundary layer where we always find positive values which contribute to the dissipation of mean kinetic energy. In the North Hadley region the pressure gradient force is negative in the lower troposphere which indicates a sink for mean kinetic energy in this region of convergence; the pressure gradient force gives a positive contribution in the upper troposphere indicating a source for mean kinetic energy in this region of divergence.

In the monsoon region it is known that the motion field exibits large convergence in the lower troposphere and divergence in the upper troposphere, this being driven by the latent heat release. This pattern together with a negative horizontal pressure gradient force indicates that the lower troposphere is a sink of the mean

Table 6.3 Mean kinetic energy budget within each pressure bounded layer in June-August in the tropical region (35N-25S)

Unit: $erg/cm^2 sec$

Pressure layer (mb)	$\frac{\partial \bar{K}}{\partial t}$	$\frac{\partial(\bar{u}\bar{K})}{\partial x} + \frac{\partial(\bar{v}\bar{K})}{\partial y}$	$\frac{\partial}{\partial p}(\bar{\omega}\bar{K})$	$\bar{u}\left(\frac{\partial \overline{u'u'}}{\partial x} + \frac{\partial \overline{u'v'}}{\partial y}\right) + \bar{v}\left(\frac{\partial \overline{u'v'}}{\partial x} + \frac{\partial \overline{v'v'}}{\partial y}\right)$	$g\left(\bar{u}\frac{\partial \bar{z}}{\partial x} + \bar{v}\frac{\partial \bar{z}}{\partial y}\right)$	$\bar{u}\bar{F}_x + \bar{v}\bar{F}_y$
100-150	-1.38	-21.9	-14.2	9.7	-8.2	-36.0
150-200	-1.91	-64.8	32.8	23.3	8.6	-1.9
200-300	-2.58	-118.0	158.0	62.4	99.1	199.0
300-400	-1.06	-28.3	-48.2	39.1	-14.7	-53.1
400-500	-0.55	-1.4	-79.8	13.8	-72.5	-140.0
500-700	-0.46	-1.3	-52.5	5.8	-94.3	-143.0
700-850	-0.09	0.8	1.8	-1.1	-26.7	-25.3
850-1000	-0.01	0.1	2.1	-1.0	-184.0	-183.0

Table 6.4 Mean kinetic energy budget within each pressure bounded layer in June-August in the North Hadley region (35N-05N)

Unit: $erg/cm^2 sec$

Pressure layer(mb)	$\frac{\partial \bar{K}}{\partial t}$	$\frac{\partial(\bar{u}\bar{K})}{\partial x} + \frac{\partial(\bar{v}\bar{K})}{\partial y}$	$\frac{\partial(\bar{\omega}\bar{K})}{\partial p}$	$\bar{u}\left(\frac{\partial \overline{u'u'}}{\partial x} + \frac{\partial \overline{u'v'}}{\partial y}\right) + \bar{v}\left(\frac{\partial \overline{u'v'}}{\partial x} + \frac{\partial \overline{v'v'}}{\partial y}\right)$	$g\left(\bar{u}\frac{\partial \bar{z}}{\partial x} + \bar{v}\frac{\partial \bar{z}}{\partial y}\right)$	$\bar{u}\bar{F}_x + \bar{v}\bar{F}_y$
100-150	-2.54	9.8	10.7	6.7	-114.0	-89.5
150-200	-3.88	34.1	-0.7	11.3	-138.0	-97.3
200-300	-5.80	23.5	2.4	20.2	-35.5	4.8
300-400	-2.98	-0.5	-15.9	7.3	6.5	-5.5
400-500	-1.66	-2.4	-12.0	-0.3	5.5	-10.9
500-700	-1.41	-0.9	-1.7	-2.8	24.3	17.4
700-850	-0.23	-1.6	5.4	-1.3	4.9	7.1
850-1000	-0.08	-3.2	11.9	-0.2	-198.0	-190.0

Table 6.5 Mean kinetic energy budget within each pressure bounded layer in June-August in the South Hadley region (05N-25S)

Unit: $erg/cm^2 sec$

Pressure layer(mb)	$\frac{\partial K}{\partial t}$	$\frac{\partial(\bar{u}\bar{K})}{\partial x}+\frac{\partial(\bar{v}\bar{K})}{\partial y}$	$\frac{\partial(\bar{\omega}\bar{K})}{\partial p}$	$\bar{u}\left(\frac{\partial\overline{u'u'}}{\partial x}+\frac{\partial\overline{u'v'}}{\partial y}\right)$ $+\bar{v}\left(\frac{\partial\overline{u'v'}}{\partial x}+\frac{\partial\overline{v'v'}}{\partial y}\right)$	$g\left(\bar{u}\frac{\partial\bar{z}}{\partial x}+\bar{v}\frac{\partial\bar{z}}{\partial y}\right)$	$\bar{u}\bar{F}_x+\bar{v}\bar{F}_y$
100-150	0.15	-48.3	-32.6	12.9	94.8	26.9
150-200	0.55	-131.0	45.3	33.0	100.0	48.2
200-300	1.30	-212.0	266.0	92.3	165.0	313.0
300-400	1.19	-45.9	-68.2	60.5	-33.3	-85.8
400-500	0.76	0.1	-129.0	22.9	-134.0	-239.0
500-700	0.64	-2.1	-86.3	10.6	-198.0	-275.0
700-850	0.06	0.4	3.9	-0.9	-58.4	-54.9
850-1000	0.02	0.6	0.3	-1.4	-165.0	-166.0

Table 6.6 Mean kinetic energy budget within each pressure bounded layer in June-August in the monsoon region (25N-05N, 10E-170E) Unit: $erg/cm^2 sec$

Pressure layer(mb)	$\frac{\partial K}{\partial t}$	$\frac{\partial(\bar{u}\bar{K})}{\partial x}+\frac{\partial(\bar{v}\bar{K})}{\partial y}$	$\frac{\partial(\bar{\omega}\bar{K})}{\partial p}$	$\bar{u}\left(\frac{\partial\overline{u'u'}}{\partial x}+\frac{\partial\overline{u'v'}}{\partial y}\right)$ $+\bar{v}\left(\frac{\partial\overline{u'v'}}{\partial x}+\frac{\partial\overline{v'v'}}{\partial y}\right)$	$g\left(\bar{u}\frac{\partial\bar{z}}{\partial x}+\bar{v}\frac{\partial\bar{z}}{\partial y}\right)$	$\bar{u}\bar{F}_x+\bar{v}\bar{F}_y$
100-150	-1.71	40.5	-33.8	10.5	-252.0	-169.0
150-200	-3.00	109.0	-61.7	7.9	-347.0	-295.0
200-300	-5.23	86.2	-36.6	3.2	-289.0	-241.0
300-400	-2.73	8.4	20.6	-1.2	-64.4	-39.3
400-500	-1.42	0.3	12.2	-2.2	-38.5	-29.6
500-700	-1.11	-3.1	-10.0	-3.1	9.8	-7.5
700-850	-0.13	-17.9	79.3	0.3	42.3	32.5
850-1000	-0.08	-12.2	33.7	1.1	-174.0	-151.0

kinetic energy and the upper troposphere is a source of the mean kinetic energy. This idea has been pointed out by Starr (1948).

The vertical integral of the mean kinetic energy budget is presented in Table (6.7). It is observed that the mean kinetic energy dissipation is larger in the South Hadley region(05N-25S) where the value is 433 ergs/cm^{2}sec than in the North Hadley region where the value is 363 ergs/cm^{2}sec. This may due to the larger mean kinetic energy in the South Hadley region than in the North Hadley region. It is expected that there will be large mean kinetic energy dissipation in a region which contains a large mean kinetic energy.

Table 6.7 Vertical integral of mean kinetic budget in June-August at various region Unit: erg/cm^{2}sec

	$\frac{\partial \bar{K}}{\partial t}$	$\frac{\partial(\bar{u}\bar{K})}{\partial x}+\frac{\partial(\bar{v}\bar{K})}{\partial y}$	$\frac{\partial(\bar{\omega}\bar{K})}{\partial p}$	$\bar{u}\left(\frac{\partial \overline{u'u'}}{\partial x}+\frac{\partial \overline{u'v'}}{\partial y}\right)$ $+\bar{v}\left(\frac{\partial \overline{u'v'}}{\partial x}+\frac{\partial \overline{v'v'}}{\partial y}\right)$	$g\left(\bar{u}\frac{\partial \bar{z}}{\partial x}+\bar{v}\frac{\partial \bar{z}}{\partial y}\right)$	$\bar{u}\bar{F}_x+\bar{v}\bar{F}_y$
tropic (35N-25S)	-8.0	-234.8	00	152.0	-292.2	-383.0
North Hadley cell (35N-05N)	-18.6	58.8	00	33.6	-444.3	-363.9
South Hadley cell (05N-25S)	4.7	-438.2	00	230.9	-228.9	-433.0
Monsoon region (25N-05N, 10E-170E)	-15.4	211.2	00	16.5	-1112.0	-900.0

In the tropical region (35N-25S) the mean kinetic energy dissipation is balanced by the horizontal pressure gradient force combined with horizontal transport across the boundaries. The vertical intergral of the gradient of vertical transport $\frac{\partial}{\partial p}(\bar{\omega}\bar{K})$ is zero as expected. In the North Hadley region the horizontal pressure gradient force is the only important term to maintain the mean kinetic energy dissipation. In the South Hadley region the main contribution to maintain the mean kinetic energy dissipation is the horizontal advection, the Reynolds stress transport term and the horizontal pressure gradient force are both about one-half the size of the horizontal advection of the horizontal advection of mean kinetic energy. In the monsoon region , mean kinetic energy dissipation is as high as 900ergs $cm^{-2}sec^{-1}$. This may be due to the large mean kinetic energy content of this region as shown in Figure 6. 1. Horizontal transport is less important compared with the large horizontal pressure gradient force and the Reynolds stress transport is negligible in this region. The large horizonal pressure gradient force in the monsoon region also indicates that the large mean kinetic energy is maintained against the frictional dissipation by the horizontal pressure force. This is the same conclusion as Keshavavmurty (1970). This is quite different from the South Hadley region. The dissipation of mean kinetic energy in these region compared with Vincent (1970) are given in Table (6. 8).

Table 6.8 Mean kinetic energy dissipation for June-August in various regions.

unit : $ergs/cm^2sec$

region	35N-25S	35N-05N	05N-25S	Monsoon region (25N-05N, 10E-170E)
present studies	383	364	433	900
regios	30N-30S	30N-00N	00N-30S	
vincent's result	740	384	1100	

The eddy kinetic energy dissipation according to Oort (1964) is ten times large than the mean kinetic energy dissipation for the whole Northern Hemisphere from annual means. Dutton and Johnson (1967) obtained the mean kinetic energy and the eddy kinetic energy dissipation values of 550 $ergs/cm^2sec$ and 5850$ergs/cm^2sec$ respectively also indicating that the eddy kinetic energy dissipation is about ten times larger than the mean kinetic energy dissipation for the Northern Hemisphere from annual means. Is this ratio still true in the tropics? The eddy kinetic energy dissipation also can be calculated as the residue term in the eddy kinetic energy budget, as given by:

$$\int \left(\overline{u'F_{x'}} + \overline{v'F_{y'}} + \overline{u^*}\,\overline{F_x^*} + \overline{v^*}\,\overline{F_y^*} \right) dm$$

and we wish to calculate this in future studies.

CONCLUSIONS

The present studies are confined to June-August in the tropical region. From the result of a comparison of the continuity equation and the first law of thermodynamics both used to evaluate $\bar{\omega}$ we found that the second one is not a good method. The adiabatic method, neglecting diabatic heating in the first law of thermodynamics, can't be used to evaluate $\bar{\omega}$ in the tropics. All the large scale vertical motion used in this study are derived from the continuity equation.

A large vertical motion over the monsoon region generate an intense Walker cell with the center of the cell close to 80E. It is also suggested that the two wave pattern in the extratropical region in June-August is generated by the dynamical deflection of the zonal current passing over mountains. In the horizontal transport the Ω-angular momentum is assumed to be zero across any latitude circle but is one or two orders of magnitude larger than the relative angular momentum transport in any limited regions in the tropics. The largest southward transport of Ω-angular momentum is found in the Indian monsoon region. The vertical transport of angular momentum across a given pressure level is mainly due to the Ω-angular momentum transport. The largest vertical transport of angular momentum in the tropical region in June-August is located at monsoon regions.

The mean kinetic energy of the whole column of atmosphere in

the monsoon region is about 4×10^8 ergs/cm^2 which is four times larger than other regions at the same latitude in the tropical region. The large mean kinetic energy in the monsoon region is primarily maintained by the horizontal pressure gradient force against the large mean kinetic energy dissipation. The mean kinetic energy dissipation in the monsoon region is about 900 ergs cm^{-2} sec^{-1} which is larger than the mean kinetic energy dissipation for the whole tropical region, the latter value being about 340 ergs cm^{-2} sec^{-1}.

REFERENCES

Ananthakrishnan R., Chelam E.V., Ramakrishnan A.R. and Thiruvengadathan A., 1967: Some dynamical aspects of the zonal and meridional circulations over India and neighbourhood. Dynamics of Lange-Scale Atmospheric Processes, Proceeding of the International Symposium, 424-449.

Bolin B., 1950: On the influence of the earth's orography on the general character of the westerlies. Tellus, 2, 184-195.

Burger A.P., 1958: Scale consideration of plantary motions of the atmosphere. Tellus, 10, 195-205.

Davis P.A., 1963: An analysis of the atmosphere heat budget. J. Atmos. Sci., 20, 5-21.

Dutton J.A. and Johnson D.R., 1967: The theory of available potential energy and a variation approach to atmosphere energetics. Advanced in Geophysics, 12, New York, Academic Press, 333-436.

Holopainen E.O., 1963: On the dissipation of kinetic energy in the atmosphere. Tellus, 15, 26-32.

Katayama A., 1966: On the radiation budget of the troposphere over the Northern Hemisphere (I). J. Met. Soc. Japan, 44, 381-401.

Katayama A., 1967: On the radiation budget of the troposphere over the Northern Hemisphere (II) and (III). J. Met. Soc. Japan, 45, 1-39.

Keshavamurty R. N., 1968: On the maintainance of the mean zonal motion in Indian summer monsoon. Mon. Wea. Rev., 96, 23-31.

Kesgavamurty R. N. and Awade S. T., 1970: On the maintenance of the mean monsoon trough over north India. Mon. Wea. Rev., 98, 315-320.

Kidson J. W., Vincent D. G. and Newell R. E., 1969: Observation studies of the general circulation of the tropics: long term mean values. Quart. J. Roy. Meteor. Soc., 95, 258-287.

Kidson J. W. and Newell R. E., 1969: Exchange of atmospheric angular momentum between the hemisphere. Nature, 221, 352-353.

Kung E. C., 1966a: Kinetic energy generation and dissipation in the large-scale atmospheric circulation. Mon. Wea. Rev., 94, 67-82.

Kung E. C., 1966b: Large scale balance of kinetic energy in the atmosphere. Mon. Wea. Rev., 94, 627-640.

Kung E. C., 1969: Further study on the kinetic energy balance. Mon. Wea. Rev., 97, 573-581.

Kyle A., 1970: Longitudinal variation of large scale vertical motion in the tropics, Master thesis, Department of Meteorology, M. I. T.

Manabe S. and Smagorinsky J., 1967: Simulated climatology of a general circulation model with a hydrologic cycle, (II) Analysis of the tropical atmosphere. Mon. Wea. Rev., 95, 155-169.

Newell R.E., Kidson J.W. and Vincent D.G., 1970: The general circulation of the tropical atmosphere and interaction with extra-tropical latitudes (to be published by M.I.T. Press).

Oort A.H., 1964: On estimates of the atmosphere energy cycle. Mon. Wea. Rev., 92, 483-493.

Oort A.H. and Rasmusson E.M., 1970: On the annual variation of the monthly mean meridional circulation. Mon. Wea. Rev., 98, 423-442.

Palmen E.H., 1959: On the maintenance of kinetic energy in the atmosphere. The atmosphere and the sea in motion, Rockefeller Institute Press, New York, 212-224.

Smith P.J., 1969: On the contribution of a limited region to the global energy budget. Tellus, 21, 202-207.

Starr V.P., 1948: On the production of kinetic energy in the atmosphere. J. Meteor., V, 193-196.

Starr V.P., 1951: A note on the eddy transport of angular momentum. Quart. J. Roy. Met. Soc., 77, 44-50.

Troup A.J., 1965: The 'southern oscillation'. Quart. J. Roy. Met. Soc., 91, 490-506.

Vincent D.G., 1970: Seasonal changes in the global atmospheric energy balance and results for restricted regions. Ph.D. dissertation, Department of Meteorology, M.I.T.

Walker G.T. and Bliss G.T., 1932: World Weather V. Mem. Roy. Met. Soc., 4, 53-84.

World Weather Records 1966: Environmental Data Services, ESSA, U.S. Department of Commerce Vol. 1-6.

ACKNOWLEDGEMENTS

The writer is most grateful to his advisor, Professor Reginald E. Newell, for his advice and encouragment throughout this study. He also thanks Drs. G. J. Boer and D. G. Vincent for their helpful suggestions and discussions. Thanks are also due to Miss Yu-chih C. Chiang for typing the thesis and to Miss Isabelle Kole for drawing the figures. The computations, data collection and analysis have been supported by the U. S. Atomic Energy Commission under contract AT (30-1) 2241